2008

Development of a high-throughput fermentation assay using colorimetric measurement of gas production

Steven Bly
Iowa State University

Development of a high-throughput fermentation assay using colorimetric measurement of gas production

by

Steven Thomas Bly

A thesis submitted to the graduate faculty

in partial fulfillment of the requirements for the degree of

MASTER OF SCIENCE

Co - majors: Agricultural Engineering; Biorenewable Resources and Technology

Program of Study Committee:
Robert Anex, Major Professor
D. Raj Raman
Brent Shanks

Iowa State University

Ames, Iowa

2008

TABLE OF CONTENTS

LIST OF TABLES

LIST OF FIGURES

ACKNOWLEDGEMENTS

I would like to thank all of the people that have helped me to be successful during my graduate career with their guidance, advice, and constant support.

My advisor, Dr. Robert Anex, has been a motivator for completion of my graduate studies. His guidance and advice throughout the duration of my research was quite useful and necessary for the success of this research. Dr. Raman's advice and assistance was valuable and I greatly appreciate his positive remarks and encouragement along the way. I would also like to thank Alex Deutmeyer for his assistance in development of the image acquisition software for my research.

My fellow graduate students in our laboratory, Asli Isci, Jenni Himmelsbach, and Pat Murphy have been a pleasure to work with and know. They were always willing to assist me with my research and offer valuable advice. I especially want to acknowledge Pat Murphy for being a good friend and the best mentor I had at Iowa State. Pat helped ease my transition to graduate school, taught me the methods and importance of experimental research, and helped renew my intellectual ambition that I occasionally lost track of along the way.

Most importantly, I would like to thank my many friends and family for their constant support of my studies at Iowa State. Their encouragement has made the journey through graduate school a valuable and rewarding experience.

ABSTRACT

Typical methods for determining ethanol production from biomass feedstocks involve the use of High Performance Liquid Chromatography (HPLC) or Gas Chromatography (GC). Such methods require expensive instruments and the time required to process a large number of samples can delay experimental campaigns and process development. The object of this study was to develop a simple, high-throughput, low-cost ethanol assay using CO_2 as a surrogate for ethanol production during fermentation. A chemi-visual sensor was developed based on visually measuring color change due to pH in a buffered indicator solution separated from the fermentation chamber by a CO_2-permeable membrane.

Carbon dioxide was introduced into the fermentation chamber of the chemi-visual sensor while the pH and red-green-blue (RGB) color values of the phenol red indicator solution were recorded. A CCD camera (WebCam) and image analysis software package developed in Matlab® was used to record the RGB values of the chemi-visual solution at each CO_2 loading. Calibration curves were developed for the following relationships: CO_2 vs. pH, pH vs. RGB, and CO_2 vs. RGB.

The chemi-visual sensor solution was used to monitor CO_2 production in a series of glucose fermentations. The CCD camera recorded the RGB signal and samples of the fermentation broth were taken throughout the experiments. The use of green signal change in the chemi-visual solution as a predictor for ethanol production can account for approximately 92% of the change in actual ethanol content for real-time ethanol production values. Multiple fermentations were conducted in order to calibrate the chemi-visual sensor and to characterize the accuracy of ethanol predictions. It was determined that it would be most appropriate to use this sensor as a predictor of final ethanol production values since

dynamic effects of fermentation kinetics, gas transfer, and green signal variability make predictions of real-time ethanol values less reliable.

CHAPTER 1.

GENERAL INTRODUCTION

Objectives

The primary objective of this research was to develop and characterize a low-cost system to measure carbon dioxide gas produced during fermentation as a surrogate for ethanol production. A secondary objective was to evaluate the potential to miniaturize the sensing system to allow the monitoring of a large number of fermentations simultaneously.

Literature Review

The U.S. Renewable Fuel Mandate requires fuel producers to produce at least 36 billion gallons of renewable fuel by the year 2022 (The White House, 2008). Of those 36 billion gallons, 16 billion gallons are required to originate from cellulosic feedstock sources such as switchgrass, wood wastes, or corn stover. Screening of lignocellulosic feedstocks, cellulosic enzymes, new fermentation organisms, and their combinations for optimum fermentability is going to become increasingly important as the use of cellulosic feedstocks is developed in order to meet the mandated fuel production requirement set forth by the U.S. government.

There have been many methods evaluated for determining the ethanol yields in fermentations. High Performance Liquid Chromatography (HPLC) is one of the most commonly used methods for determining ethanol concentrations. The use of HPLC is described in an article by Dien et al. (2002) where the fermentation of five different Bt hybrids of corn were evaluated for ethanol production.

In a different approach, Weimer et al. (2005) describe an ethanol yield assay that is based on measuring the pressure in the head space above an ethanol fermentation. Ethanol yields were correlated with concurrent measurements of ethanol concentration by gas chromatography. Masini et al. (1999) used a similar approach and described the measurement of carbon dioxide production as a means to analyze yeast cell metabolism. The carbon dioxide production was sensed by measuring pressure above the fermentations. Ankom Technology (Macedon, NY) has developed a commercially available system with pressure sensor modules that are used to monitor gas production of microbial systems in a laboratory setting. In another approach, Zor et al. (2007) describe a biosensor that is used for real-time monitoring of glucose and ethanol in fermentations.

Duguid et al. (2007) screened different biomass physiological components to determine the sugar content and ethanol processing characteristics. In the study, wheat stover was physically separated into chaff, leaves, nodes, and internodes. The glucose and xylose concentrations were determined by HPLC. All fractions were subjected to an alkaline pretreatment coupled with enzyme hydrolysis and an acid pretreatment with simultaneous saccharification and fermentation (SSF). HPLC analysis was used to analyze the lignocellulosic sugars available after the acid pretreatment step. The ethanol concentration was determined by use of the assay described by Weimer et al. (2005) where the head space gas pressure was used as a surrogate for ethanol production. Other assays have been proposed to allow the rapid screening of biomass feedstock using correlations between easily measured compositional characteristics and ethanol yield or biochemically available carbohydrates (Isci et al. 2008, Murphy et al. 2007).

Previous research has also attempted to measure ethanol production by measuring carbon dioxide, a by-product of the fermentation reaction. A relatively simple method is described by Varga et al. (2004) in which the carbon dioxide produced during fermentation is weighed in order to determine ethanol yield. The results were well correlated with ethanol measurements obtained by HPLC.

Herber et al. (2005) describe the concept of using a miniaturized sensor with a gas permeable membrane to detect partial pressure of carbon dioxide levels in stomachs. In another medical application, Severinghaus et al. (1958) describe a carbon dioxide sensor that uses a gas permeable membrane of Teflon to measure partial pressure of oxygen and carbon dioxide in blood.

Digital imaging has been used in a wide range of biological research applications. The use of a charged-coupled device (CCD) camera for enumeration of marine viruses is described by Chen et al. (2000). In the study, CCD images of fluorescently stained microbes are processed and used to asses the amount of microbes present in a marine environment. This is in substitution for transmission electron microscopy (TEM) measurements which are more expensive and time-consuming. Although the microbial counts found by digital image analysis were higher than direct counts, Chen et al. state that the use of digital images can facilitate the counting of a higher number of viruses for a given amount of microscope time.

Feng et al. (2007) utilize a CCD camera to monitor the fermentation of barley tempeh. Barley tempeh is fermented by use of the fungus *Rhizopus oligosporus*. As the barley tempeh fermentation was conducted, images were taken, and samples were taken and analyzed for ergosterol concentration with HPLC. Image processing software was used to statistically analyze the image color (hue, saturation, and luminescence). It was found that

the use of images allows for a rapid and non-intrusive method to monitor the status of the barley tempeh fermentation process.

The use of Fourier transform infrared (FTIR) spectroscopy for monitoring ethanol fermentations is described by Veale et al. (2007). In the study, a simple glucose fermentation was conducted while FTIR measurements of glucose and ethanol concentrations were correlated with ethanol and glucose concentrations measured by HPLC. The FTIR measurements were made using a Bio-Rad FTS 6000 spectrophotometer (Cambridge, MA) and an ATR flow cell. The researchers demonstrated the potential use of FTIR spectroscopy for on-line fermentation monitoring and/or process control.

In an attempt to monitor titrations colorimetrically, Gaiao et al. (2006) developed a digital-image based titration. Gaiao et al. used a CCD digital camera as a detection device for titration by recording the RGB values of a titrated solution containing color-based pH indicators. The webcam and the color-based sensing solution were placed in a white box in order to obtain uniform illumination. A correlation was obtained between color (RGB) and titrant added.

The purpose of the experiments described in this thesis is to develop a system to detect carbon dioxide from ethanol fermentations colorimetrically by use of a buffered indicator solution and CCD camera.

Thesis Organization

The information presented in this thesis is organized into five chapters. The first chapter contains a statement of thesis organization, objectives, and review of the relevant literature. Chapter 2 contains a paper titled “Development of a high-throughput fermentation

assay using colorimetric measurement of gas production" intended for journal publication. The third through fifth chapters provide supporting data and information. The third chapter describes the experiments conducted during the proof-of-concept of the chemi-visual sensor design. The fourth chapter describes the selection of buffer concentration for glucose fermentation experiments. Chapter 4 also contains results of an experiment to analyze the response of the camera system using alternating current (AC) and direct current (DC) light sources. The fifth chapter presents the development of the system used to monitor pressure in the fermentation experiments. The sixth chapter provides general conclusions of the experiments and suggestions for future work.

References

Abbaspour, A., Mehrgardi, M.A., Norri, A., Kamyabi, M.A., Khalafi-Nezhad, A., Rad, M.N.S. 2006. Speciation of iron(II), iron(III) and full-range pH monitoring using paptode: Asimple colorimetric method as an appropriate alternative for optodes. Sensors and Actuators B. 113: 857-865

Beuvink J.M.W., Spoelstra S.F. 1992. Interactions between substrate, fermentation end-products, buffering systems and gas production upon fermentation of different carbohydrates by mixed rumen microorganisms in vitro. Appl. Microbiol Biotechnol. 37: 505-509

Chitrakar, S. 2002. Quantifying corn deterioration by use of CO_2 –sensitive gel. MS Thesis. Bangkok, Thailand: Asian Institute of Technology, School of Environment Resources and Development

Dantigny, P. 1995. Modeling of the aerobic growth of *Saccharomyces cerevisiae* on mixtures of glucose and ethanol in continuous culture. Journal of biotechnology. 43: 213-220

Dien, B.S., Bothast, R.J., Iten, L.B., Barrios, L., Eckhoff, S.R. 2002. Fate of Bt protein and influence of corn hybrid on ethanol production. Cereal Chem. 79:582-585

Feng, X.M., Olsson, J., Swanberg, M., Schurer, J., Ronnow, D. 2007. Image analysis for monitoring the barley tempeh fermentation process.. Joutnal of Applied Microbiology. 103:1113-1121

Gaiao, E.N., Martins, V.L., Lyra, W.S., Almeida, L.F., Silva, E.C., Araujo, M.C.U. 2006. Digital image-based titrations. Analytica Chimica Acta. 570:283-290

Herber, S., Bomer, J., Olthuis, W., Bergveld, P., van den Berg, A. 2005. A Miniaturized Carbon Dioxide Sensor Bases on Sensing of pH-Sensitive Hydrogel Swelling with a Pressure Sensor. Biomedical Microdevices. 7(3): 194-204

Isci, A., Murphy, P., Anex, R. 2008. A rapid simultaneous saccharification and fermentation (SSF) technique to determine ethanol yields. Bioenergy Research. 1 163-169

Masini, A., Batani, D., Previdi, F., Milani, M., Pozzi, A., Turcu, E., Huntington, S., Takeyasu, H. 1999. Yeast cell metabolism investigated by CO_2 production and soft X-ray irradiation. The European Physical Journal-Applied Physics. 5: 101-109

Murphy, P., Moore, K., Raman, D.R. 2007. Carbohydrate availability assay for determining lignocellulosic biomass quality. ASABE Paper No. 077077. St. Joseph, Mich.: ASABE

Severinghaus J.W., Bradley A.F. 1958. Electrodes for Blood pO_2 and pCO_2 Determination. J. Appl. Physiol. 13: 515-520

Suzuki, H., Kojima, N., Takei, F., Ikegami, K., Tamiya, E., Karube, I. 1989. Fabrication of a Microbial Carbon Dioxide Sensor Using Semiconductor Fabrication Techniques. Electroanalysis. 1: 305-309

Uttamial, M., Walt, D.R. 1995. Fiber Optic Carbon Dioxide Sensor for Fermentation Monitoring. Biotechnology. 13: 597-601

Varga, E., Klinke, H.B., Reczey, K., Thomsen, A.B. 2004. High Solid Simultaneous Saccharification and Fermentation of Wet Oxidized Corn Stover to Ethanol. Biotechnology and Bioengineering. 88(5): 567-574

Weimer, P.J., Dien, B.S., Springer, T.L., Vogel, K.P. 2005. In vitro gas production as a surrogate measure of the fermentability of cellulosic biomass to ethanol. Appl Microbiol Biotechnol 67:52-58

The White House. Energy. Available at: www.whitehouse.gov/infocus/energy. Accessed 25 March 2008.

Zor, K., Gaspar, S., Hashimoto, M., Suzuki, H., Csoregi, E. 2007. High Temporal Resolution Monitoring of On-Line Amperometric Flow-Through Microdetector. Electroanalysis. 19(1): 43-48

CHAPTER 2.

DEVELOPMENT OF A HIGH-THROUGHPUT FERMENTATION ASSAY USING COLORIMETRIC MEASUREMENT OF GAS PRODUCTION

A paper to be submitted to *Bioresource Technology* for publication

S.T. Bly, R.P. Anex, D.R. Raman, B. Shanks

Introduction

There are several methods available to monitor ethanol production during fermentation. One of the most commonly used methods is High Performance Liquid Chromatography (HPLC). Other methods measure carbon dioxide evolution as a surrogate for ethanol. A relatively simple method is described by Varga et al. (2004) in which the carbon dioxide (CO_2) produced during fermentation is weighed in order to determine ethanol yield. Weimer et al. (2005) describe an ethanol yield assay based on estimating CO_2 evolution by measuring pressure in the head space above ethanol fermentations.

In an attempt to monitor titrations colorimetrically, Gaiao et al. (2006) developed a digital-image based titration. Gaiao et al. used a CCD digital camera as a detection device for titration by recording the RGB values of a titrated solution that was supplemented with color-based pH indicators.

Since common methods of measuring ethanol such as HPLC are relatively slow andexpensive, there is a need for a simple, high-throughput, low-cost ethanol assay. The sensor that is described could be useful for screening of lignocellulosic feedstocks, cellulosic enzymes, new fermentation organisms, and their combinations for optimum fermentability

that will become increasingly important as the use of cellulosic feedstocks is developed in order to meet the mandated cellulosic fuel production.

Methods

Concept

The basis for the design of the chemi-visual sensor relies on the stoichiometric relationship between ethanol and carbon dioxide production from the fermentation of sugars such as glucose and xylose which may be derived from starch or cellulosic material. The functionality of the sensor relies on the ability to detect CO_2 production as a surrogate for ethanol produced during sugar fermentation. For example, one mole of glucose is fermented by yeast to produce two moles of ethanol and two moles of carbon dioxide (Figure 2.1).

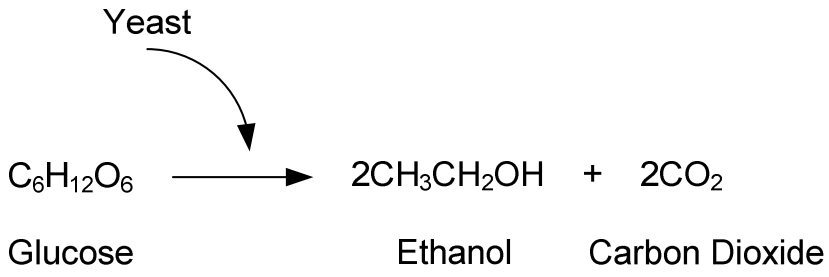

Figure 2.1: Conversion of glucose into ethanol and carbon dioxide by yeast fermentation

The chemi-visual sensor described here consists of a buffered indicator with color-based pH indicator that absorbs the CO_2 produced during fermentation. A gas-permeable membrane supports the indicator solution above the fermentation headspace to allow separation between the indicator solution and fermentation broth while also allowing gas transfer into the indicator solution. The CO_2 causes a pH decrease in the indicator solution

that in turn causes a color change in the indicator solution. The color change is sensed by a CCD camera, and quantified in software.

A buffered indicator solution is used in the sensing system. Equipment to validate the sensing system was designed and built. An experiment was designed to develop calibrations for the interactions between: pH of indicator solution and volume CO_2 added, color change and pH of indicator solution, color change and volume CO_2 added. Experiments were conducted to determine the effect of mass transfer limitations due to the membrane and diffusion of CO_2 into the indicator solution on the responsiveness of the sensor. The chemi-visual sensor was used to predict ethanol production of glucose fermentations.

Apparatus

A 125 mL Erlenmeyer flask was modified for use in fermentation monitoring experiments. A gas-permeable membrane, Fluorpore Membrane Filter – FGLP04700 was used to support a buffered indicator solution above the fermentation headspace. A #15 glass o-ring joint (V.M. Glass Company) was fused to the top of the flask and the bottom of the indicator solution tube. Initial fermentations indicated that a simple spring-loaded o-ring clamp was not adequate to hold the pressures generated during fermentations and leaking of the indicator solution was observed. A more robust clamp was designed and fabricated out of Delrin, a hard plastic, to hold the o-ring joints together (Figure 2.2).

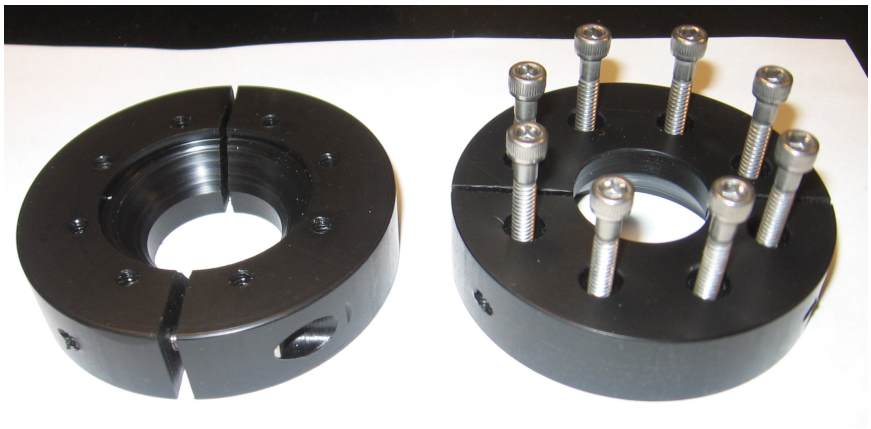

Figure 2.2: Clamp used to hold glass o-ring joints together

A stainless steel ball bearing with a diameter of 3/8” was placed in the solution on top of the membrane in order to break up the gaseous boundary layer at the membrane-liquid interface.

A sampling port with valve was fused near the base of the flask to enable sampling of fermentation broth. The valve was located below the level of the fermentation broth to ensure that no gas would escape due to sampling (Figure 2.3).

A Logitech Webcam (Model: QuickCam Pro 4000) was positioned at a distance of 1 inch from the pH-color indicator solution tube. The webcam was interfaced with a personal computer and the Image Acquisition software in MATLAB was used to monitor the red, green, and blue (RGB) pixel values as a function of time. RGB data were the average of all values within a specified viewing area (100 pixels x 100 pixels) at a constant location of the indicator solution. The RGB values were measured at a frequency of 1 Hz and recorded data were the average computed every 60 seconds.

Pressure transducers from MSI Sensors (Part No. 1210A-100D-3L) were used to measure the pressure above the fermentation headspace and above the headspace of the

indicator solution. The pressure measurements were recorded at a frequency of 1Hz and averaged every 60 seconds.

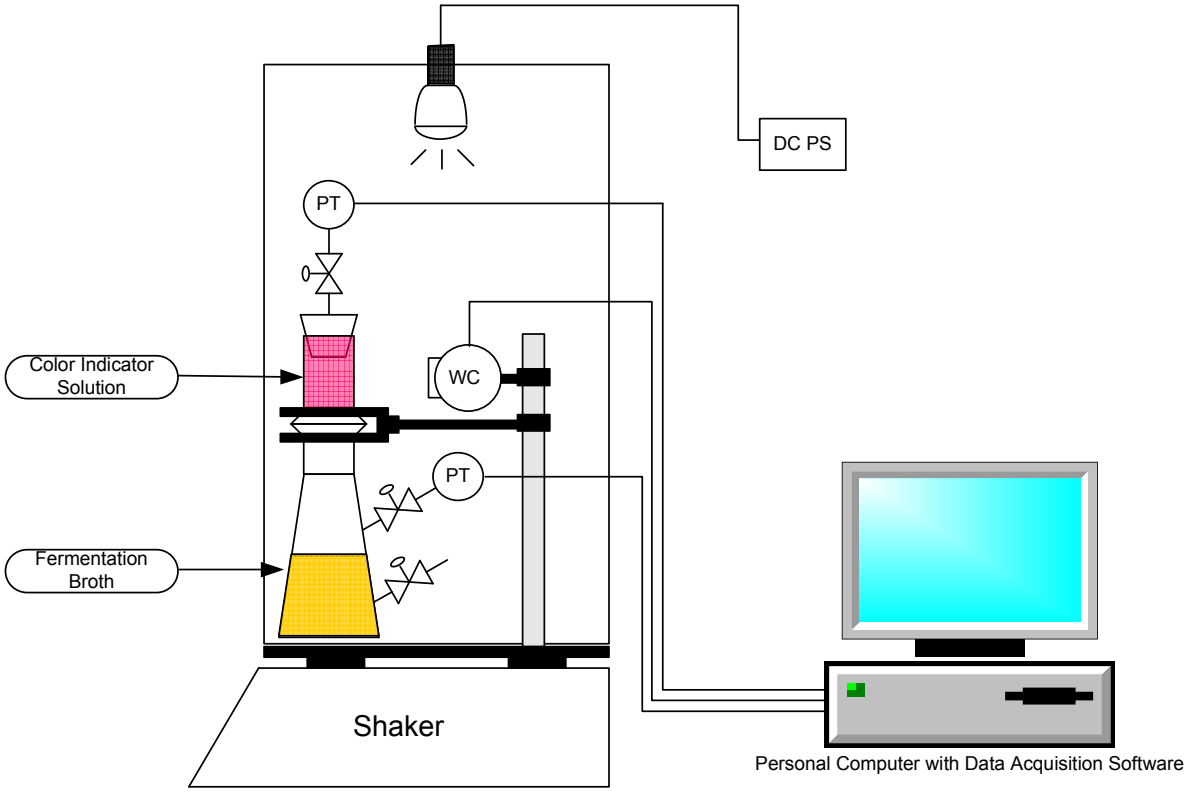

Figure 2.3: Testing apparatus for fermentation monitoring (PT: pressure transducer, WC: webcam, DC PS: 12 V direct current power supply)

The webcam and chemical indicator solution apparatus were supported on the table of a New Brunswick Scientific C1 Platform Shaker. A box was built out of white foam poster board with a thickness of ¼". The box was designed to sit on the shaker table and surround the sensing apparatus to provide uniform illumination. The dimensions of the box were 11" (l) x 13" (w) x 20" (h). A 12 Volt /1.4 watt DC LED lamp (Sunlite Manufacturing, Brooklyn, NY) was used as the light source. A lid was made out of the same material that was modified to allow the insertion of the 1.4 W LED lamp. The base of the shaker table was

also covered with a layer of white paper in order to reduce variation due to reflection from the moving metal surface of the shaker platform.

Indicator Solution for First Calibration

Triethanolamine (TEA) buffer solution was the first buffer chosen for use in the indicator solution. Titration of the TEA buffer solution with CO_2 gas showed that the pH changed from approximately 8.0 to 6.6 over the range of CO_2 evolution expected from the planned glucose fermentation experiments. Phenol red indicator was chosen because it changes from red to yellow between pH = 8.0 and pH =6.6. The indicator solution was prepared at room temperature (25^{o}C) and comprised of: 16.3 mM Triethanolamine Buffer Solution (Sigma-Aldrich, St. Louis, MO, U.S.), 30 µM phenol red, and de-ionized water. A single batch of buffered indicator solution was used for all experiments using that buffer and was stored in a refrigerator at 8^{o}C.

Procedure

Initial Calibration

The chemi-visual sensing system was titrated with small amounts of CO_2-rich gas in order to verify the assumed relationships behind the sensor concept. CO_2-rich gas was added to the headspace below the gas-permeable membrane and allowed to dissolve into the indicator solution. The pH of the indicator solution and the corresponding RGB values were measured for each level of CO_2 addition. The green signal of the RGB value was found to have the largest response to the pH change and was chosen to be used as the color parameter of interest. For small amounts of CO_2, linear relationships were found between the following: pH and CO_2 added, Green signal and pH, and green signal and CO_2 added.

The results of the initial experiments suggest that the sensor can detect CO_2 addition at small levels. However, lab-scale glucose fermentations were estimated to produce about 300 mL of CO_2. The sensor is required to detect these higher levels of CO_2 that are observed during lab-scale fermentations.

Glucose Fermentation

A simple spreadsheet was designed to calculate the expected ethanol and CO_2 production for given substrate loadings. The amount of CO_2 used in the initial proof-of-concept experiments was significantly lower than that observed in typical laboratory fermentation experiments. An indicator solution with greater buffer capacity was prepared for sensor experiments with typical fermentation substrate loading. The indicator solution was prepared with 0.1 M TEA, 30 µM phenol red, and de-ionized water.

Fermentation Broth

The fermentation medium contained 20 g/L peptone, 10 g/L yeast extract, 50 mM citric acid buffer. Red Star baker's yeast was the fermentation organism used in all fermentation experiments. In order to evaluate the utility of the sensor for varied substrate loadings, two different glucose and yeast loadings were chosen to achieve differing fermentation kinetics. These will be referred to as the "high" and "low" glucose loadings. The high glucose loading included 16.0 g/L glucose and 1.47 g/L yeast. The low glucose loading included 8.0 g/L glucose and 4.0 g/L yeast. These loadings were chosen through numerical simulation of ethanol fermentation using the model outlined in Chapter 5 of this thesis. The "low glucose loading" transient was formulated with a high yeast loading to give a rapid transient response with lower final ethanol concentration. The "high glucose loading" conditions were selected to produce a slower transient with a higher final ethanol

concentration. These two cases allow a comparison of the chemi-visual sensor's response to different fermentation kinetics and final ethanol production levels. The fermentations were conducted at 37^{o}C while the broth was shaken. The CCD camera was used to observe the color change in the solution while samples of fermentation broth were taken at time intervals appropriate to each glucose loading. The fermentation samples were analyzed for ethanol content by HPLC and correlated with the change in green signal observed by the CCD camera.

Results and discussion

Glucose Fermentation

The change in green signal observed in the chemi-visual sensor tracked the ethanol transients of the high glucose loading fermentations as shown in Figure 2.4. Note that the change in green signal in RGB scale units corresponds to the left axis and the ethanol concentration in g/L corresponds the right axis in Figure 2.4.

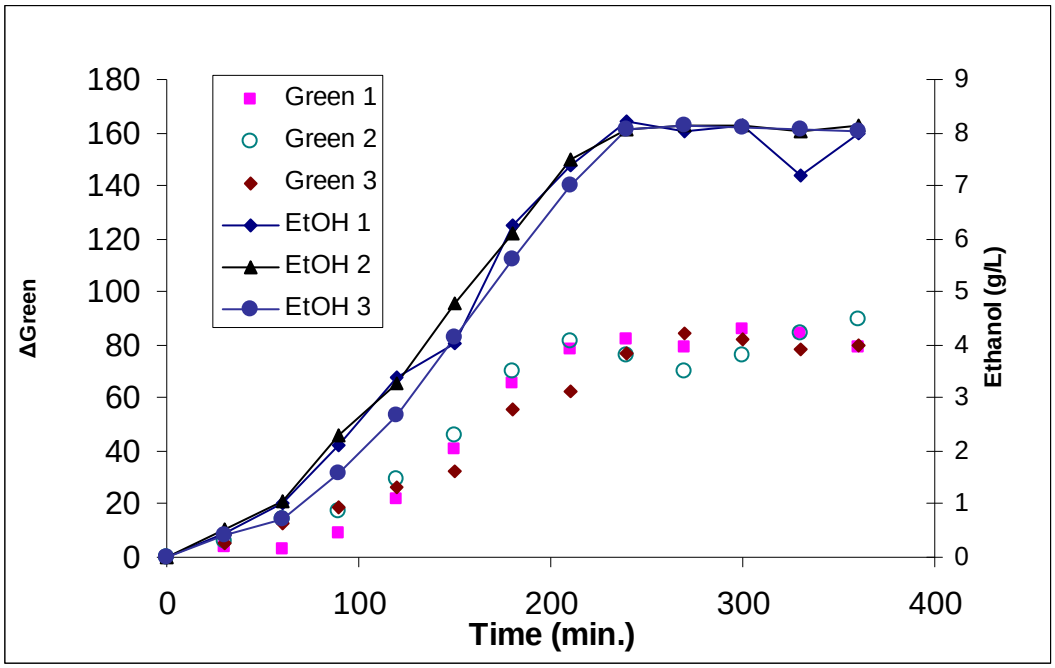

Figure 2.4: Ethanol production and green signal response of high glucose loading fermentation (16 g/L Glucose) with TEA buffer indicator

The sensor response to the low glucose loading transient is shown in Figure 2.5. It is expected that the green signal response to a fermentation with higher ethanol production would be higher than the green signal response for a fermentation with lower ethanol production. The average ethanol produced in the low substrate loading experiments was measured via HPLC as 54.6% of the ethanol produced in the high substrate loading experiments. Therefore, it is expected that the green signal observed in the fermentation with low substrate loading would also be approximately 50% of the green signal response realized in the fermentation with high substrate loading. However, the green signal realized in the low substrate loading experiments was 143% of the green signal observed during the with high substrate loading experiments. A large amount of variation was also observed in the green signal during the lower substrate loading experiments.

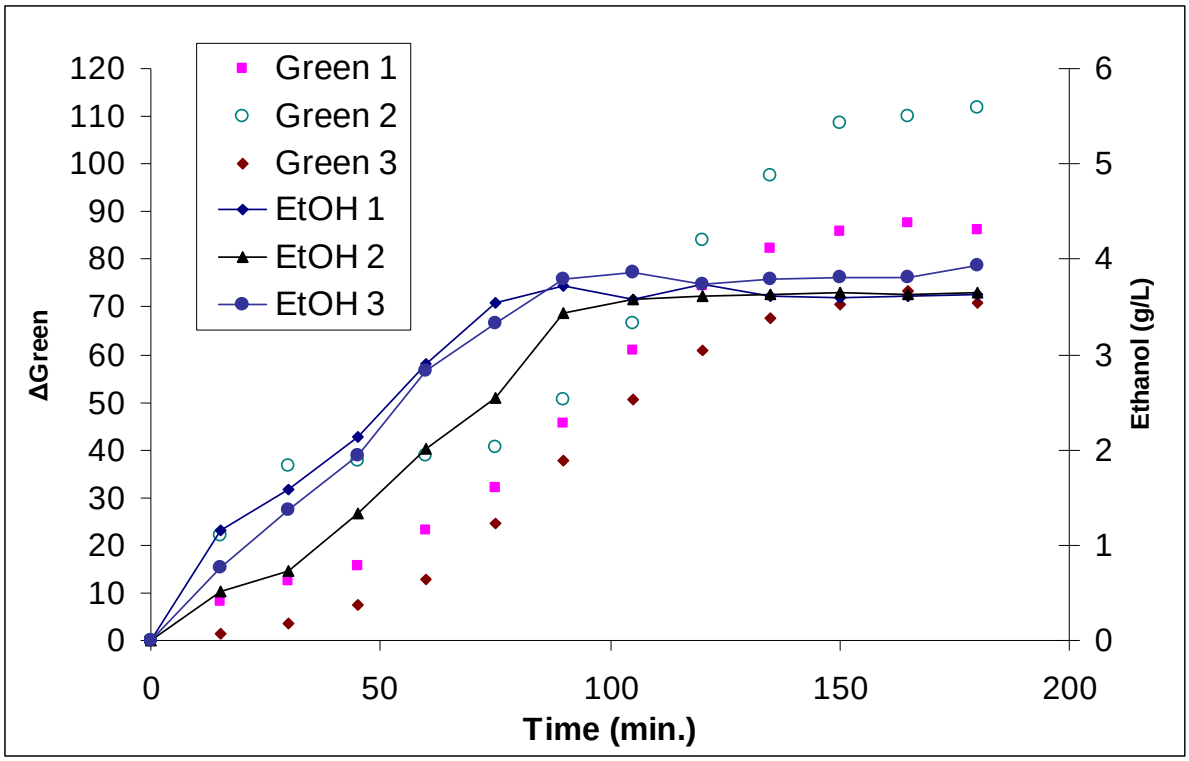

Figure 2.5: Ethanol production and green signal response of low glucose loading fermentation (8.0 g/L Glucose) with TEA buffer indicator

These counter-intuitive results lead us to investigate possible explanations for the highly non-linear sensor response to CO_2 production. One possible cause for the non-linearity of green signal response is the nature of the TEA buffer. TEA is used industrially as a CO_2 absorbent. TEA buffer absorbs carbon dioxide forming stable carbamate through an exothermic reaction that is slow relative to the rapid acid-base reactions that involve relatively weak ionic bonding (Sotelo, et al., 2004, Hook, 1997, Danckwerts, et al., 1967). Absorption of CO_2 by the TEA through several different pathways complicates the response of the sensor reducing the predictability and repeatability of the sensor response due to multiple types of reactions with varying time constants.

With this in mind, an indicator solution with a simple phosphate buffer system was developed. A phosphate buffer was prepared with disodium phosphate (Na_2HPO_4 @ 0.0897 M) and monosodium phosphate (NaH_2PO_4 @ 0.0103 M). The pH was adjusted to approximately 8.0 by the addition of sodium hydroxide (0.005625 M).

Glucose Fermentations with Phosphate Buffer Indicator

Glucose fermentations were conducted using the same substrate, yeast, and nutrient loadings as described earlier for the "low" and "high" substrate loading experiments. The indicator solution used was 18 mL phosphate buffer with 30 µM phenol red indicator. The CCD camera was used to observe color change and samples of the fermentation broth were taken at regular time intervals and analyzed for ethanol concentration using HPLC.

The two fermentations were designed to achieve different levels of CO_2 production. The fermentations were also designed to produce ethanol at different rates. It was anticipated that observing the green signal response for fermentations with different kinetics would reveal any time-delay in the response due to limitations of gas transfer into the indicator solution. It was also expected that differing levels of CO_2 production would reveal differences in response due to saturation of CO_2 in the indicator solution, or loading related mass transfer limitations . The measured ethanol concentrations from two replications of each transient are shown in Figure 2.6.

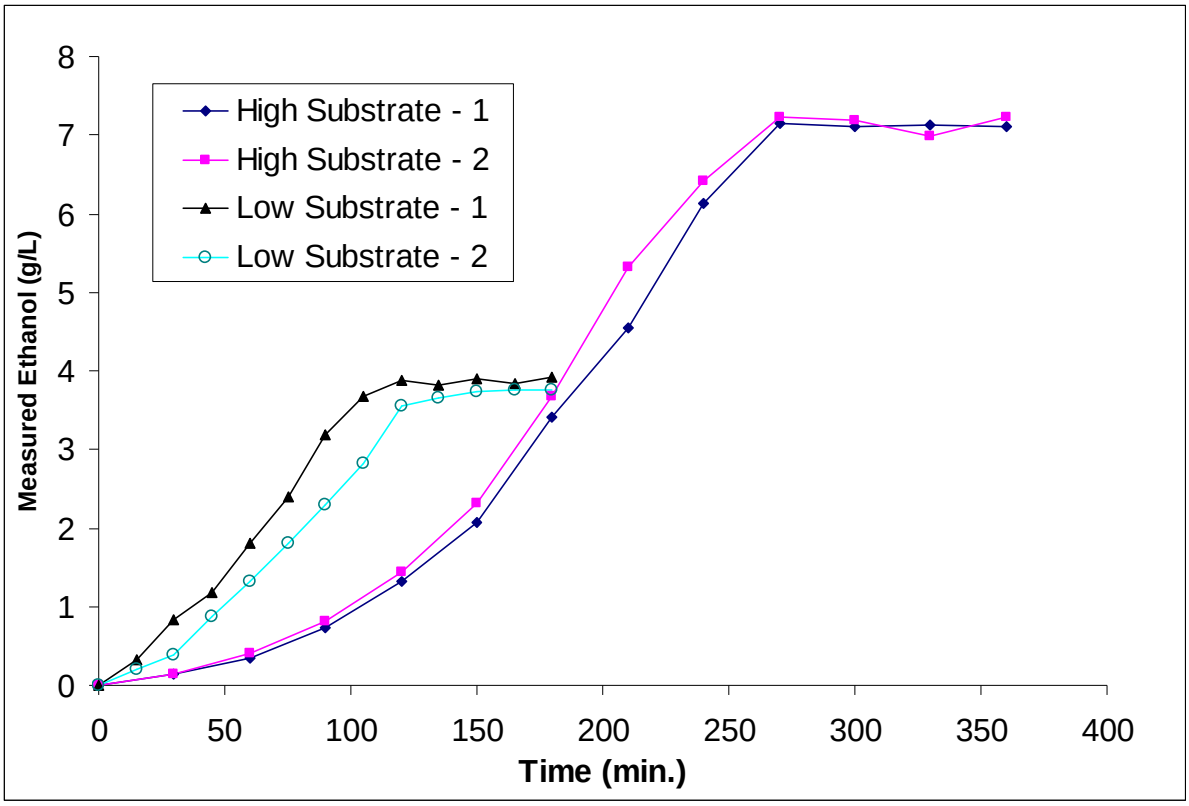

Figure 2.6: Ethanol production vs. time for fermentations at different kinetics

The observed green signal and ethanol concentration for the high substrate loading experiments are shown in Figure 2.7. The green signal response tracks ethanol production over time, but the maximum green signal is observed approximately sixty minutes before the maximum ethanol concentration. The observed ethanol concentrations in the two experiments diverge at just over 200 minutes. The corresponding green signals diverge approximately 60 minutes later. The ethanol concentration transients converge to similar values approximately 270 minutes into the experiment, but the observed green signals to not converge. This indicates that there is a lag of approximately 60 minutes between the measured ethanol concentration and observed green signal and that after approximately 240

minutes, the chemi-visual sensor is no longer responsive to changes in CO_2 production. This results in the green signal peak occurring before the measured peak in ethanol concentration and the green signals from the two replicates not converging at peak their peak levels as is observed in the ethanol concentration data.

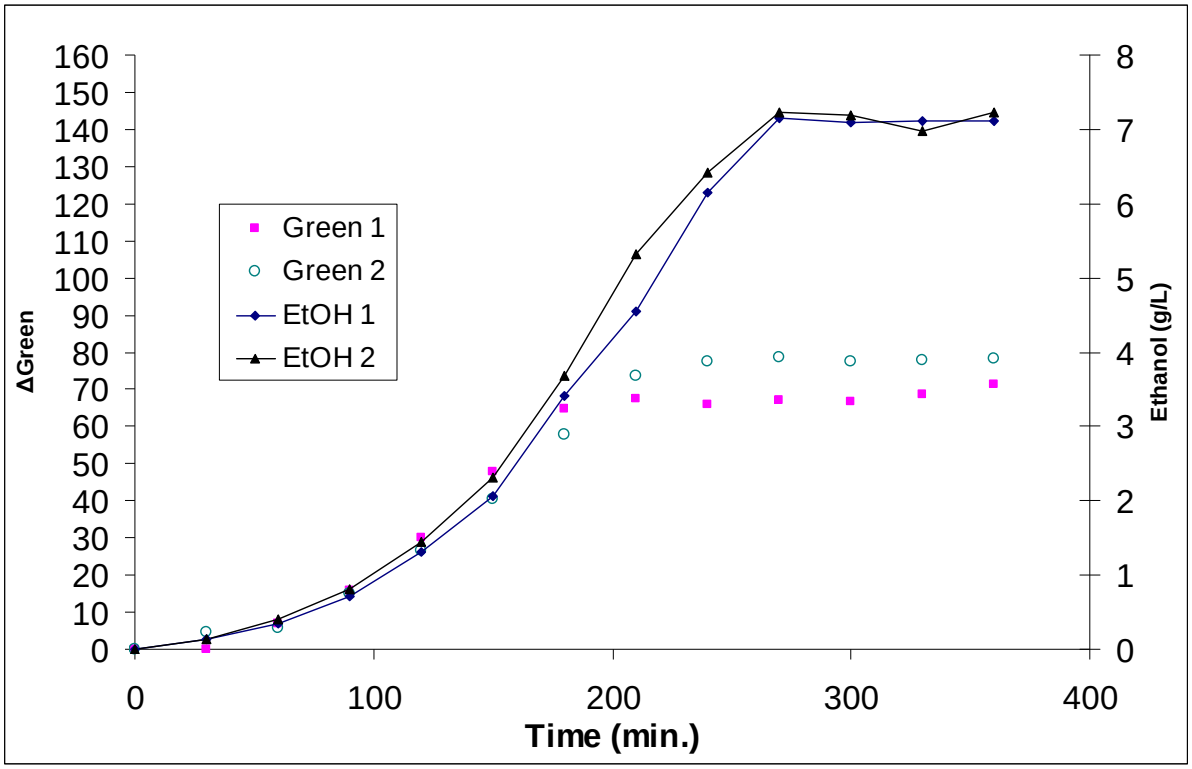

Figure 2.7: Ethanol production and green signal response of high glucose loading fermentation (16 g/L Glucose) with phosphate buffer indicator

The observed green signal and ethanol concentration for the low substrate loading experiments are shown in Figure 2.8. Early in the transient the green signal is seen to lag behind the rising ethanol concentration measurements. Again, the maximum green signal is observed prior to the ethanol concentration peak. It is plausible that the green signal lags in the beginning of the fermentation due to mass transfer limitations of the CO_2 moving through

the membrane and into the indicator solution. The ethanol produced in the low substrate loading is 53.6% of the ethanol produced of that of the high substrate loading. The green signal realized in the fermentation with low substrate loading is 67.3% of the green signal response in the fermentation with high substrate loading.

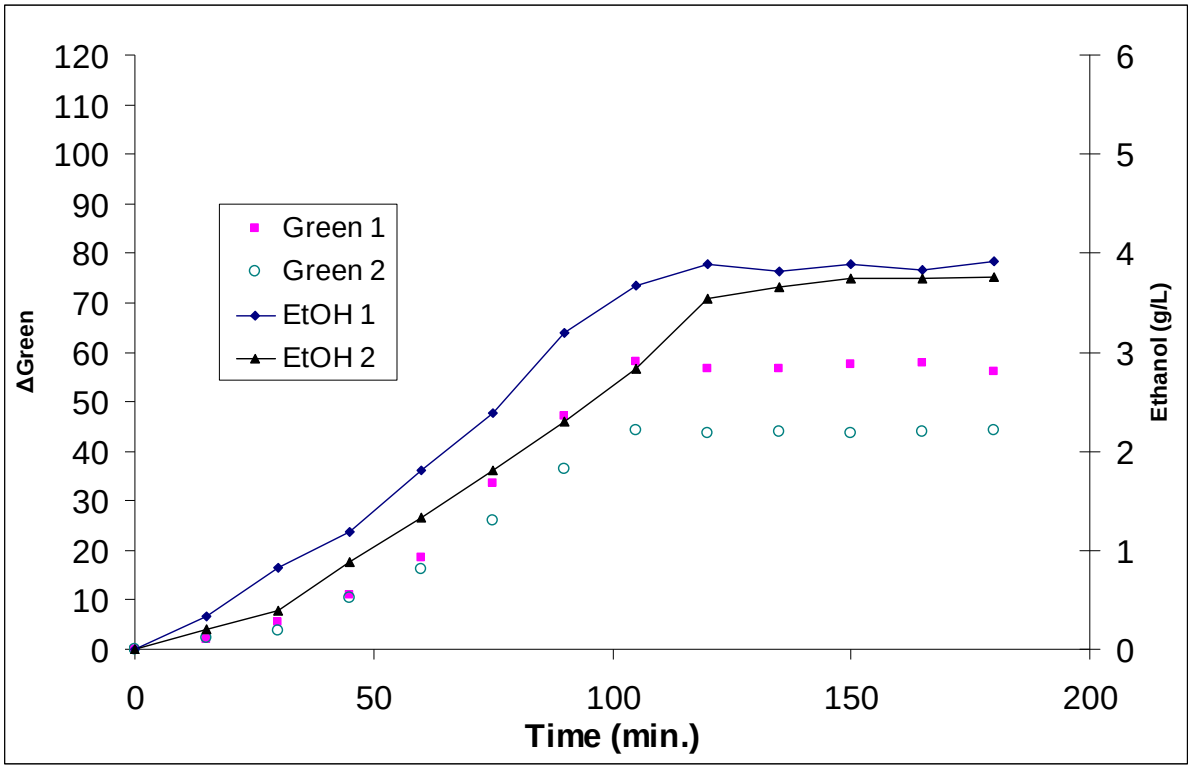

Figure 2.8: Ethanol production and green signal response of low glucose loading fermentation (8.0 g/L Glucose) with phosphate buffer indicator

Measured ethanol production values are plotted against the change in green signal in Figure 2.9 for both sets of fermentation experiments. A simple predictive model was developed by fitting a second-order polynomial to the data. The resulting model fit the data well with a correlation coefficient of 0.92 as shown on Figure 2.9.

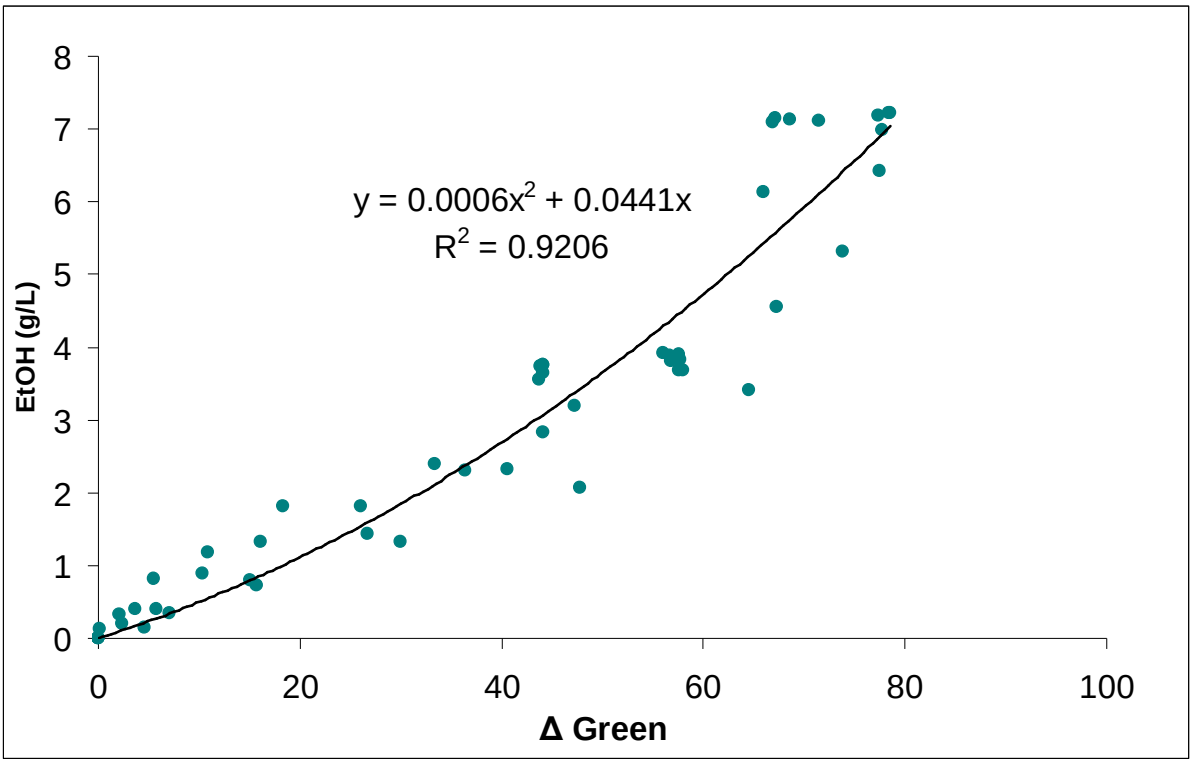

Figure 2.9: Ethanol production as a function of change in green signal (Phosphate buffer indicator)

The regression equation and correlation coefficient indicates that 92% of the variation in the actual ethanol concentration can be explained by the model. The equation shown in Figure 2.9 was used to predict ethanol concentration for the "low" and "high" substrate experiments. In Figure 2.10, predicted ethanol concentration for all four experiments is plotted against ethanol concentration measured by HPLC.

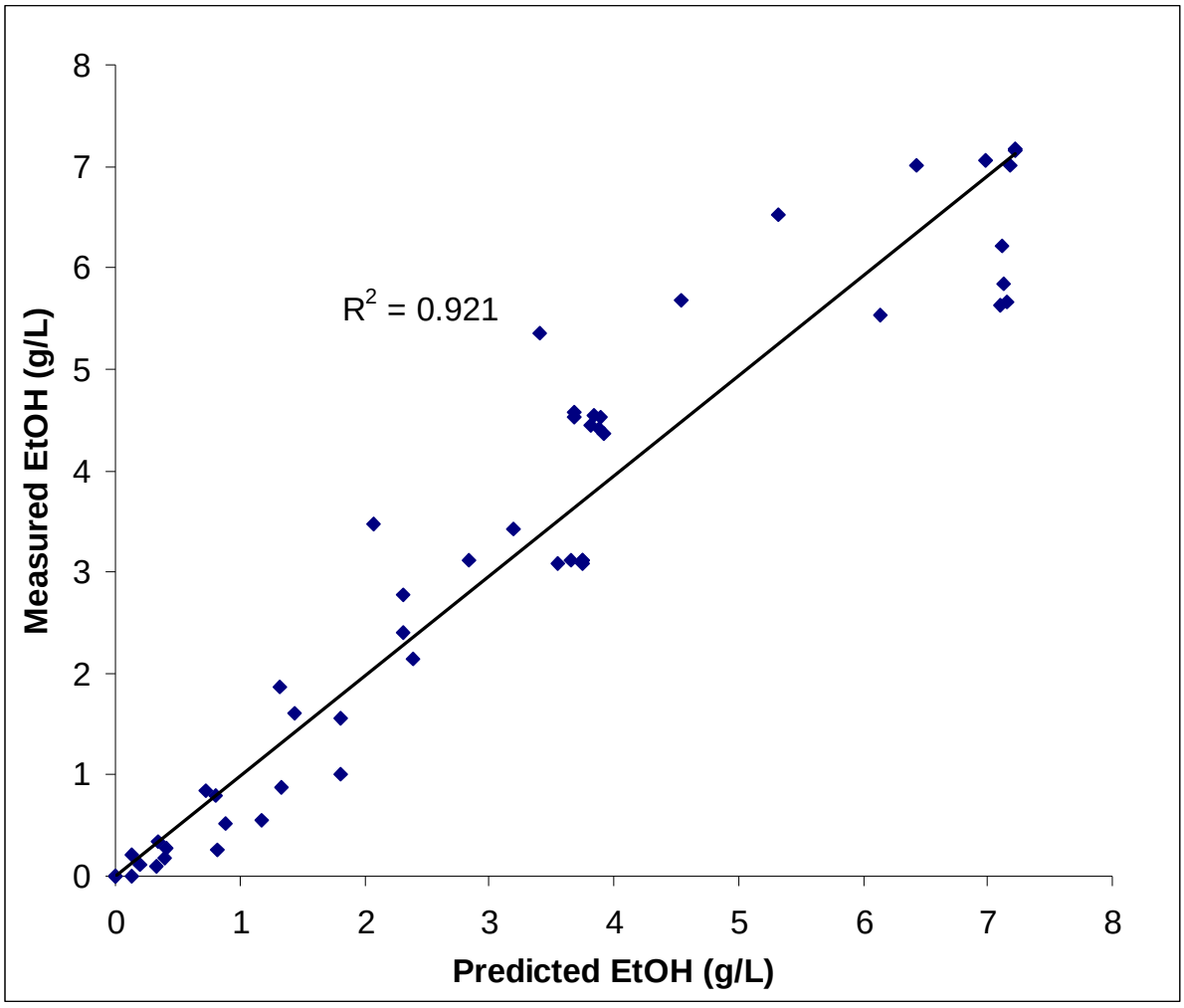

Figure 2.10: Measured ethanol production vs. ethanol predicted from calibration equation

The mean percentage error of the predictive equation was found to be 24.4%. There are many possible sources of. The CCD camera has a standard deviation of 0.38 green signal units at a static condition (Chapter 4). This standard deviation translates into only 0.02 g/L ethanol when converted using the predictive model. There may also be dynamic effects related to mass transfer of CO_2 across the membrane and absorption into the indicator solution. These factors each contribute to the uncertainty in predicted ethanol concentration.

The time lag observed and the fact that the green signal peaks before the ethanol peaks suggests that the sensor is not well suited for predicting real-time ethanol values, but may be better suited for steady-state conditions when the fermentation has completed and the ethanol concentration has stabilized. The green signal may be peaking before ethanol production is complete because there isn't a large enough pressure differential to drive the pH down as easily as when the ethanol production is lower. The observed data indicate that the sensitivity of the sensor decreases with increased CO_2 absorption. It appears that at higher ethanol concentrations, a larger change in ethanol content is required for a smaller amount of green signal change.

From Figures 2.7 & 2.8 it appeared that mass transfer of gas into the indicator solution may be affecting the performance of the sensor. An experiment was conducted in which CO_2 – rich gas was prepared and placed above the indicator solution in a sealed beaker with a pH probe used to measure pH. The objective of this experiment was simply to characterize the rate of CO_2 diffusion into the buffered indicator solution at atmospheric pressure through a gas-liquid free surface without a membrane. It is assumed that the acid-base chemistry associated with absorption of CO_2 gas into phosphate buffer is fast relative to the mass transfer of CO_2 into the solution.

CO_2 absorption into buffer solution with free surface

72 mL of phosphate buffer with phenol red indicator solution was placed in a beaker. The volume of the headspace above the buffer was determined to be 103 mL The cross-sectional area of the flask holding the indicator solution was 22.06 cm^2.

Dry ice was placed in a 250 ml beaker with approximately 10 ml of de-ionized water. Carbon dioxide (CO_2) gas was generated by allowing the dry ice to sublimate and a syringe was filled with 60 mL of CO_2 – rich gas. The CO_2 – rich gas was transferred to an empty 125 mL flask and capped for approximately two hours to allow for equilibration. 60 mL of CO_2 – rich gas was pulled from the equilibration flask and added to the headspace above the buffer solution (Figure 2.11).

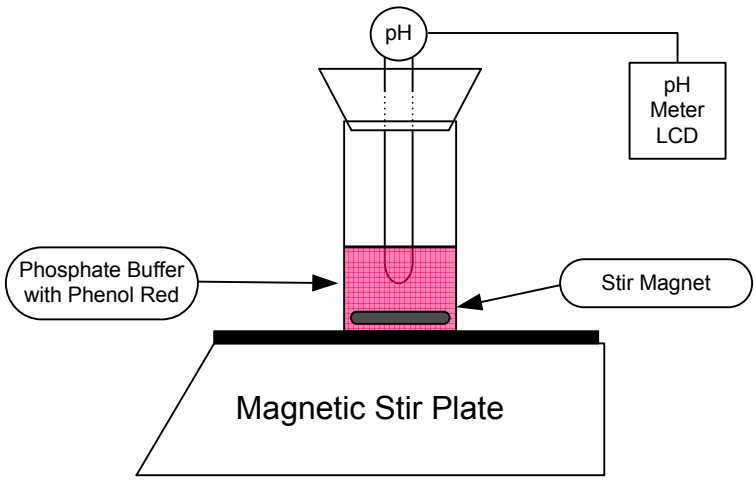

Figure 2.11: Experimental set-up for CO_2 absorption into open phosphate buffer system

The flask containing the buffer solution and CO_2 – rich gas in the headspace was capped with a rubber stopper and a pH meter was inserted into a hole in the rubber stopper to measure the pH of the buffer solution. The solution was stirred moderately with a magnet on

a magnetic stir plate while pH measurements were recorded over time. The pH was measured until the system pH leveled out and was assumed to be in equilibrium.

In order to assess the diffusion dynamics of CO_2 into the buffer it was assumed that Fick's Law for Diffusion would be applicable.

According to Smith (2004), Fick's law of diffusion for gases is defined:

$$J = D\frac{dC}{dx}$$

Where:

J = Flux (mols-cm^{-2}-s^{-1})

D = Diffusivity (cm-s^{-1})

dC/dx = Concentration gradient (mols/cm^{3})

To assess, the diffusivity, it is necessary to quantify the concentration gradient between the gas-liquid interface. Since a convenient method to assess dissolved CO_2 in the buffer was not available, a computer program, Visual MINTEQ was used to simulate system performance. Visual MINTEQ is a chemical equilibrium model for the calculation of speciation of water chemistry systems. It allows for the definition of a water chemistry system and solves for equilibrium conditions of ion speciation, pH, and partial pressures of gases at steady state equilibrium.

For our experiment, it was assumed that the buffer-gas system was in equilibrium at completion of the experiment. The final pH that was reached was assumed to be the equilibrium pH of the system. The prepared buffer solution was simulated in Visual MINTEQ by entering the molar concentrations of the phosphate buffer as described earlier.

For each pH data point that were recorded throughout the physical experiment, the amount of CO_2 added to the buffer system to result in the same steady state pH was simulated in MINTEQ. For each data point, Visual MINTEQ gave the outputs of the absorbed CO_2 concentration, pH and partial pressures of CO_2 in the headspace. Based on this information and the physical headspace volume, a mass balance on CO_2 was performed to calculate the actual partial pressure of CO_2 in the headspace of the system at each pH-time point. Fick's Law was then applied to determine the flux of CO_2 which was numerically integrated in order to determine the amount of CO_2 dissolved in the system. A diffusivity constant, D (cm/s), was calculated based on Fick's Law.

The response of pH over time for the buffer solution open to CO_2 gas is shown (Figure 2.12).

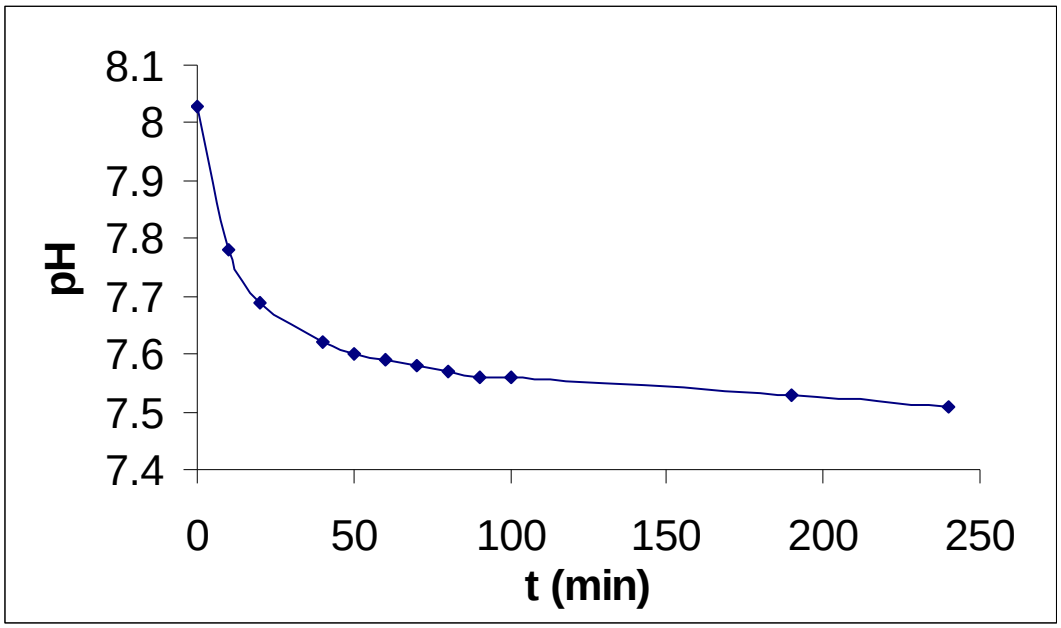

Figure 2.12: Response of pH over time for the buffer solution open to CO_2-rich gas

The response of pH over time appears to be very slow. Since it is assumed that the acid-base chemistry is relatively quick, the limitation in response time is likely caused by

mass transfer limitation of diffusion of CO_2 into the buffer solution. The response of pH to CO_2 addition in this sensor was modeled as a first-order system (Wheeler and Ganji, 2004).

$$\frac{y}{y_e} = 1 - e^{-t/\tau}$$

Where:

y = change in sensor output (pH)

y_e = equilibrium change in output of the system (pH)

t = time elapsed (s)

τ = time constant (s)

The time constant for the sensor was calculated according to the first-order reaction described based on the pH-time data for CO_2 diffusion into an open system (Figure 2.12). The time constant, τ (s), was calculated to be 18 minutes, the amount of time for the sensor to respond to 63.2% of its total response value. While assuming a time constant of 18 minutes, the amount of time required for the sensor to realize 95% of it's response was estimated to be approximately 54 minutes (~ 1 hour). For fermentation kinetics that achieve maximum ethanol (and CO_2 gas) production between 2 and 4 hours as shown previously, this sensor would not respond fast enough to characterize real-time ethanol production. Clearly this system is mass transfer limited. The amounts of dissolved CO_2 in the system were plotted and a diffusivity constant was computed (Figure 2.13).

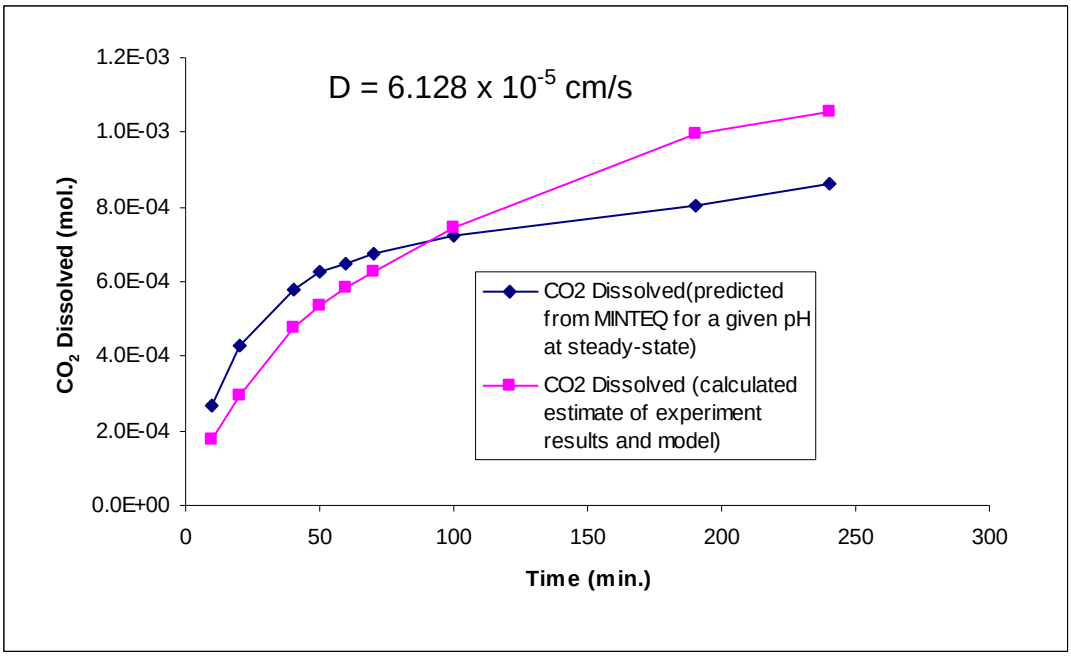

Figure 2.13: CO_2 absorption into phosphate buffer solution for open system

The plot for dissolved CO_2 that was the calculated estimate using Fick's law as described above very nearly follows the plot for dissolved CO_2 that was predicted from MINTEQ for a given pH at steady state. The plot for the estimated amount of CO_2 dissolved based on Fick's law was done using a numerical integration which led to some lack of smoothness in the plot.

Since there is clearly a mass transfer limitation due to CO_2 diffusion across the gas-liquid interface, an additional experiment was conducted to assess the difference in diffusivity between an open system and a system including a membrane at the gas-liquid interface. The objective of the described experiment was to assess any large decreases in mass transfer due the usage of the membrane.

CO_2 absorption into buffer solution with membrane present

18 ml of the phosphate buffer solution with 30 µM phenol red was placed onto the membrane and capped (Figure 2.14).

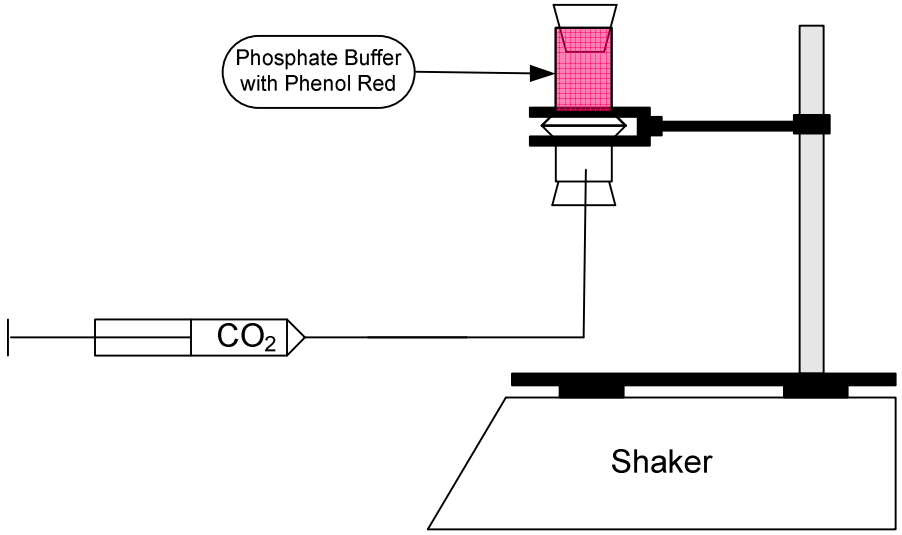

Figure 2.14: Experimental set-up for CO_2 – rich gas absorption into phosphate buffer system with membrane

A stainless steel ball bearing with a diameter of 3/8" was placed in the solution on top of the membrane in order to break up surface tension at the membrane-liquid interface. The buffered indicator solution and apparatus were supported on the table of a New Brunswick Scientific C1 Platform Shaker.

Dry ice was placed in a 250 ml beaker with approximately 10 ml of de-ionized water. Carbon dioxide (CO_2) gas was generated and a syringe was filled with CO_2 – rich gas. The CO_2 – rich gas was flushed through the length of the tubing connecting the syringe to the headspace directly below the membrane. The volume of the tubing connecting the syringe and headspace below the membrane was 10 mL. The volume of the headspace directly

below the membrane was determined to be 8 mL. The cross-sectional area of the glass tubing holding the indicator solution was 1.767 cm^2. The shaker was turned on and operated at a speed of 25 rpm. After selected time intervals, the rubber stopper above the headspace of the buffer solution was removed and the pH was recorded. The pH wasn't monitored continuously because of the errors that leakage might cause in the experiment. This was conducted at six time intervals to obtain a small dataset for pH and time.

The same analysis using MINTEQ and Fick's Law was used on the experiment with the membrane present as described earlier. The response of pH over time for the buffer solution with membrane between CO_2 gas and indicator solution is shown (Figure 2.15).

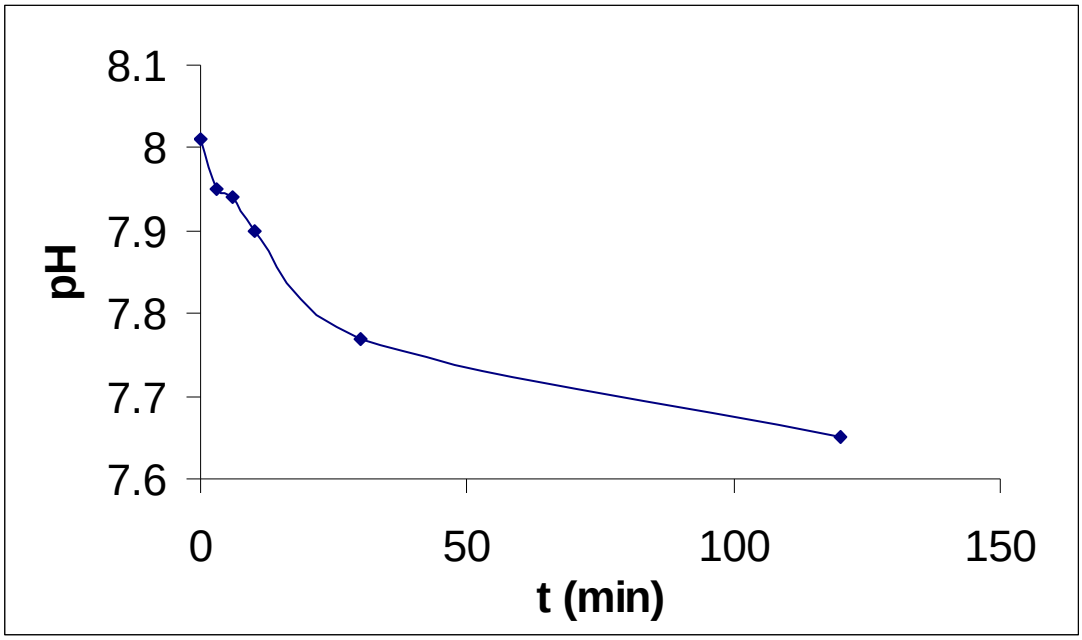

Figure 2.15: Response of pH over time for the buffer solution open to CO_2-rich gas with membrane present

Fewer data points were obtained for the case with the membrane present since the pH wasn't monitored continuously. However, the pH response of the sensor is relatively slow.

The amount of time required for the sensor to realize 95% of its response was estimated to be approximately 102 minutes.

The amounts of dissolved CO_2 in the system were plotted and a diffusivity constant was computed in order to compare with the open system (Figure 2.16).

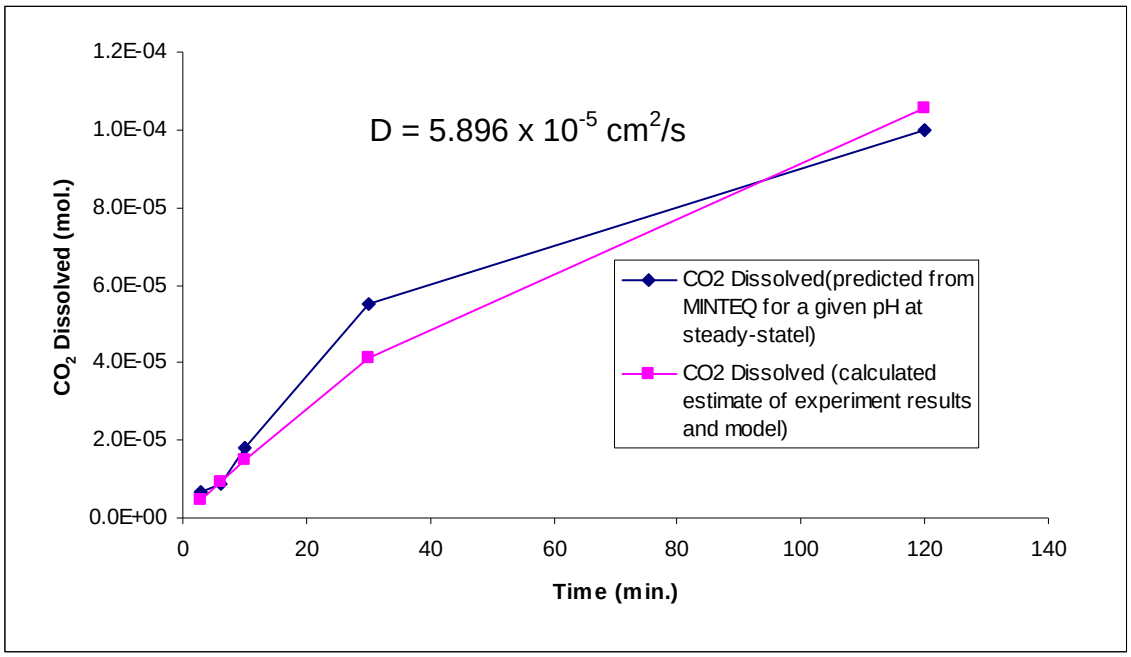

Figure 2.16: CO_2 absorption into buffer solution with membrane present

The diffusion constants found for each case are too similar to be considered different. There is also possible inherent error in the usage of the pH meter for pH values and potential errors in volume measurement and preparation of buffer solution.

If the diffusion constant for the system with the membrane was significantly lower than that of the open system, the conclusion could be made that the membrane has a significant effect on limiting gas transfer into the buffer solution. However, that is not the case. Since the diffusion constants are so similar, it can be assumed that the membrane does

not have a large effect on limiting the response time of the sensor. The limiting factor appears to be the kinetics of the gas absorption into the buffer and the effected pH change.

An additional experiment was conducted with the same design as shown in Figure 2.13 where CO_2-rich gas was placed in the headspace below the membrane and indicator solution while pH was monitored over time (Figure 2.17).

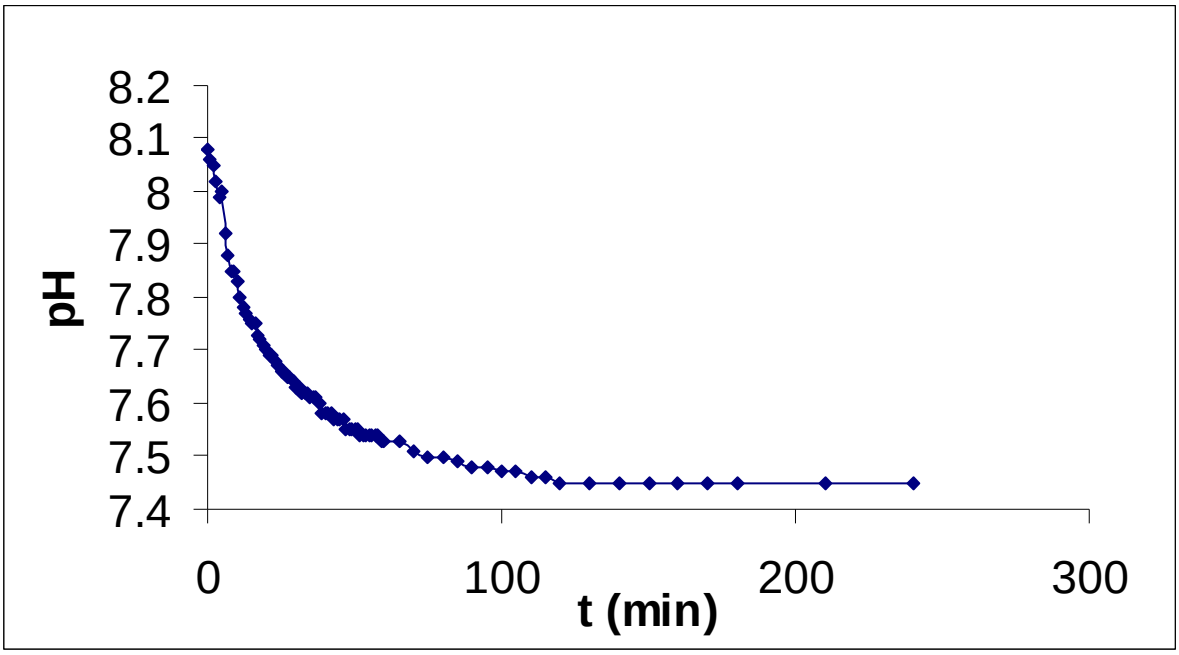

Figure 2.17: Response of pH over time for the buffer solution open to CO_2-rich gas under pressure with membrane present

The amount of time required for the sensor to realize 95% of its response was estimated to be approximately 90 minutes.

Fermentation Pressure Experiment

The data from evaluating the pressures of the fermentation headspace and the headspace above the indicator solution (found in Chapter 5) also support the hypothesis that there is minimal limitation of gas transfer due to the membrane (Figure 2.18.

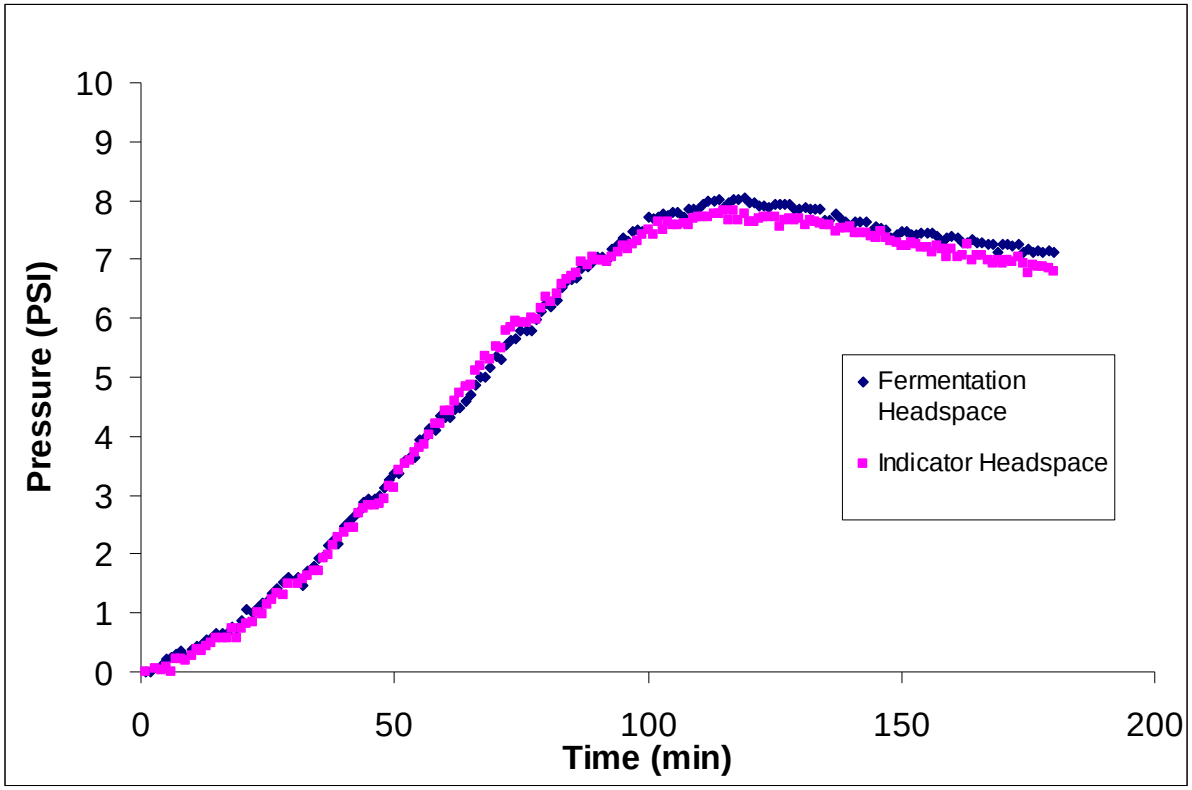

Figure 2.18: Pressure vs. time for fermentation with glucose loading of 8.0 g/L (Adjusted for volume increase due to sampling of fermentation broth)

The pressures realized on both sides of the membrane are very similar. The similarities in the pressures realized in the fermentation headspace and the headspace above the indicator solution support the hypothesis that there is no significant limitation on mass transfer of gas due to the membrane.

Modeling limits of current system with MINTEQ

MINTEQ was used to evaluate some basic limits of the existing fermentation monitoring apparatus (Figure 2.3) for sensing ethanol production from a lab-scale fermentation. The effects on three variables were considered. A realistic constraint for each value was assumed and held constant to determine the effect on the other two variables affected (Table 2.1).

Table 2.1:Output of modeling existing parameters in fermentation sensor apparatus (Note: Values indicated with an asterisk were held constant and the corresponding values in each row are the appropriate outputs)

Model Outputs		
Partial Pressure CO_2 in Headspace	Buffer pH	CO_2 Production Detected
1.50 atm *	6.3	0.170 g
0.58 atm	**6.6 ***	0.067 g
0.13 atm	6.1	**0.225 g ***

The MINTEQ model for the buffer system was used to evaluate the described in the above table and determine the effect on the related variables in the system. This analysis was conducted to test the limits of pressure, pH response and level of CO_2 detection of the current sensing system.

A reasonable limit for partial pressure of CO_2 realized in the fermentation headspace was chosen to be 1.5 atm. It is assumed that it would be unsafe to operate a fermentation in glassware at pressures higher than 1.5 atm since the flask may burst. It is also important to stay at a reasonable pressure to maintain a seal in the o-ring joints and prevent leakage of indicator solution and CO_2 gas. The buffer volume is fixed at 18 mL and the headspace volume is fixed at 50 mL to accurately represent the existing fermentation flask used for CO_2

monitoring. The terminal pH limit of 6.6 was fixed since the phenol red indicator ceases to change color below pH = 6.6 and CO_2 levels would be difficult to detect colorimetrically.

For the case when the maximum achievable partial pressure in the headspace is held constant at 1.5 atm, the buffer pH is driven to a pH of 6.3. The phenol red indicator ceases to change color below 6.6, so it would be difficult to accurately detect CO_2 absorbed colorimetrically. The detected levels of CO_2 production for the cases where headspace pressure and terminal pH of the buffer solution are fixed are 0.17 g and 0.067 g.

In previous work by Isci, et al, (2008), corn stover was fermented in a total working volume of 10 ml. The initial glucose concentration was analyzed and found to be approximately 3.0 g/L. The values of glucose loadings that this sensor is capable of are somewhat lower, but are acceptable and meet experimental standards.

The system was evaluated for fermentation with glucose loading of 3.0 g/L as in the small scale fermentations described by Isci, et al, (2008). For a glucose loading of 3.0 g/L and fermentation volume of 75 mL, the estimated CO_2 production is 0.225 g. The output of the model indicates that the pH of 6.1 would be below the minimum pH detectable by the phenol red indicator (pH of 6.6) although the partial pressure realized is small. It is observed that the highest level of CO_2 production that could be detected with the existing experimental set-up with 18 mL buffer and 50 mL of headspace is 0.067 g. This CO_2 production could be achieved with a fermentation that is within the reasonable limits of glucose loadings. For example, a fermentation with a working volume of 30 mL and glucose loading of 4.2 g/L would yield approximately 0.06 g CO_2 and could be detected by the sensor.

The results of the model for a glucose loading of 3.0 g/L are promising for the potential of scaling the system down to enable screening of multiple fermentations

simultaneously. The model output shows that a small-scale fermentation can be conducted and be detected by the sensor with a headspace volume of 50 mL and buffer volume of 18 mL. However, either the kinetics of the fermentation would have to be slower or the sensor would have to be modified to decrease the time required for pH response. A slower fermentation that would take around 24 hours to complete would likely be able to be detected by this sensor. The results indicate that it would be feasible to optimize this system for miniaturization by modifying both headspace volume and indicator solution volume.

Change in Sensor Sensitivity

The "high" and "low" substrate fermentation experiments using the phosphate buffer indicated that the sensor may be subject to mass transfer limitations. MINTEQ was used to approximate the fractions of CO_2 that are in the headspace above the fermentation and in the indicator solution. Three levels of CO_2 addition were assumed, the high and middle levels are approximately the same amounts of CO_2 evolved in the high and low substrate fermentations. The low CO_2 level was chosen arbitrarily so as to represent CO_2 production expected from a fermentation with even lower substrate loading. The results of these calculations are shown in Figure 2.19 as the number of moles of CO_2 in each compartment and percentage that is in the headspace.

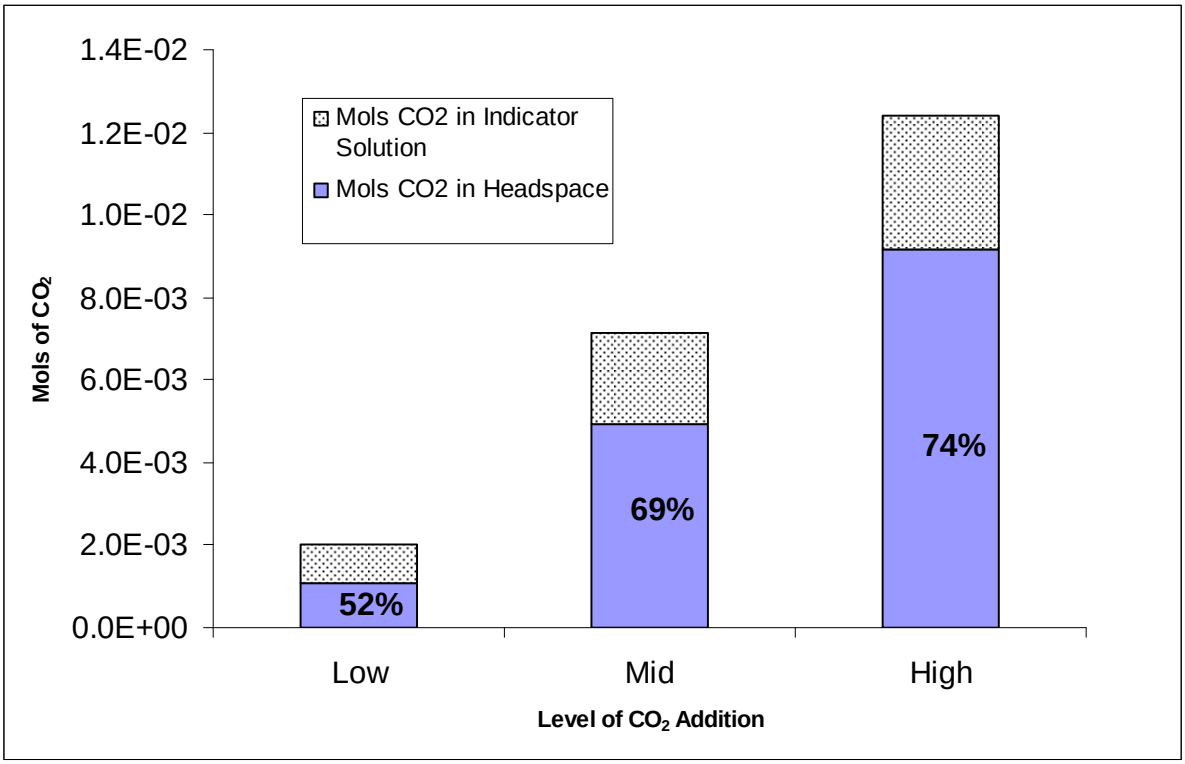

Figure 2.19: CO_2 partitioning of fermentation and indicator solution system at varied CO_2 production levels (Values are percentage of total CO_2 in the fermentation headspace, modeled in MINTEQ)

There is an increase in the fraction of total CO_2 located in the fermentation headspace with increased total CO_2. This results in an increased partial pressure of CO_2 at higher CO_2 levels. As total CO_2 production increases, an increasingly large fraction resides in the sensor headspace, which suggests that the sensor will become less sensitive to each successive mol of CO_2 produced during a fermentation. Coupled with mass transfer limitations, the response reflected by CO_2 in the indicator solution lags CO_2 levels is in the headspace and is insensitive to CO_2 produced during the tail end of a fermentation transient.

Conclusions

The use of TEA as a buffer for detecting absorption of CO_2 from ethanol fermentations was found to be non-ideal because of the unwanted side reactions and non-linearity in response to differing fermentation kinetics.

Non-linearity in the performance of the TEA buffer over different fermentation kinetics prompted the investigation of the use of a phosphate buffer. A simple phosphate buffer model coupled with experiments proved that mass transfer of CO_2 gas across the gas-liquid interface is the largest limiting factor on the response of the system.

The use of green signal change in the phosphate buffer solution as a predictor for ethanol production can account for approximately 92% of the change in actual ethanol content. It was also determined that the usage of the membrane adds no resistance to gas transfer relative to the mass transfer of CO_2 gas across the gas-liquid interface. The use of green signal poorly predicts final ethanol production values. The limitations of gas transfer into the indicator solution causes the sensor to perform poorly as a predictor for real-time ethanol values since the fermentation kinetics are dynamic and there is a significant time lag in the response of the green signal in the sensor. The indicator solution also appears to have a dynamic response to ethanol production that is also likely due to limitations in gas transfer.

More precise control of the green signal noise would likely decrease the variability in the sensor's response, and lead to more linearity in final ethanol production values with total green signal response. The recommended use for this sensor would be for a predictor of final ethanol production values since dynamic effects of fermentation kinetics, gas transfer, and green signal variability make predictions of real-time ethanol values less reliable.

References

Atkins, P. 1994. Chapter 7. In:.*Physical Chemistry*,218-219.New York, NY.: W.H. Freeman and Company

Danckwerts, P.V., McNeil, K. M. 1967. The Absorption of Carbon Dioxide into Aqueous Amine Solutions and the Effects of Catalysis. Transactions of the Institution of Chemical Engineers. 45: T32-T49

Gaiao, E.N., Martins, V.L., Lyra, W.S., Almeida, L.F., Silva, E.C., Araujo, M.C.U. 2006. Digital image-based titrations. Analytica Chimica Acta. 570:283-290

Hook, R. J. 1997. An investigation of some sterically hindered amines as potential carbon dioxide scrubbing compounds. Industrial & Engineering Chemistry Research. 36:1779-1790

Isci, A., Murphy, P., Anex, R. 2008. A rapid simultaneous saccharification and fermentation (SSF) technique to determine ethanol yields. Bioenergy Research. 1 163-169

Smith, W. 2004. Chapter 4. In:.*Foundations of Materials Science and Engineering*,158-159. New York, NY.: McGraw-Hill Publishing

Sotelo, J. L., F. J. Benitez, J. Beltran-Heredia, C. Rodriguez. 2004. R&D Note: Absorption of carbon dioxide into aqueous solutions of triethanolamine. AIChE Journal, Vol 36(8): 1263 – 1266

Varga, E., Klinke, H.B., Reczey, K., Thomsen, A.B. 2004. High Solid Simultaneous Saccharification and Fermentation of Wet Oxidized Corn Stover to Ethanol. Biotechnology and Bioengineering. 88(5): 567-574

Visual MINTEQ Ver. 2.53. Available at: http://www.lwr.kth.se/English/OurSoftware/vminteq. Accessed 8 November 2008

Weimer, P.J., Dien, B.S., Springer, T.L., Vogel, K.P. 2005. In vitro gas production as a surrogate measure of the fermentability of cellulosic biomass to ethanol. Appl Microbiol Biotechnol 67:52-58

Wheeler, A., Ganji, A. 2004. Chapter 2. In:.*Introduction to Engineering Experimentation*, 25-26. Upper Saddle River, NJ.: Pearson Prentice Hall

CHAPTER 3.

PROOF OF CONCEPT FOR CHEMI-VISUAL SENSOR DESIGN

Introduction

A buffered indicator solution was developed to be used in the sensing system. Equipment to validate the sensing system was designed and built. An experiment was designed to develop calibrations for the interactions between: pH of indicator solution and volume CO_2 added, color change and pH of indicator solution, color change and volume CO_2 added. The chemi-visual sensor was used to predict ethanol production of glucose fermentations.

Methods

Apparatus

A gas-permeable membrane, Fluorpore Membrane Filter – FGLP04700 was used to support a buffered indicator solution above the gas headspace. The membrane filters had a diameter of 45 mm. Glass o-ring joints (size #15) from V.M. Glass Company were used to hold the membrane in place. A simple clamp was used to hold the o-ring joints together. Since the inside diameter of the o-ring joints was 15 mm, the effective diameter of the membrane in contact with indicator solution and gaseous headspace was 15 mm.

An Accumet Basic AB15/15+ pH meter was used to record the pH of the indicator solution at each carbon dioxide concentration. The rubber stopper used to seal the top of the sensing apparatus was modified to allow the insertion of the pH meter's electrode into the pH-color indicator solution.

A Logitech Webcam (Model: QuickCam Pro 4000) was positioned at a distance of 1 inch from the ph-color indicator solution tube. The webcam was interfaced with a personal computer and the Image Acquisition software in MATLAB was used to capture the red, green, and blue (RGB) pixel values as a function of time (Figures 3.1, 3.2).

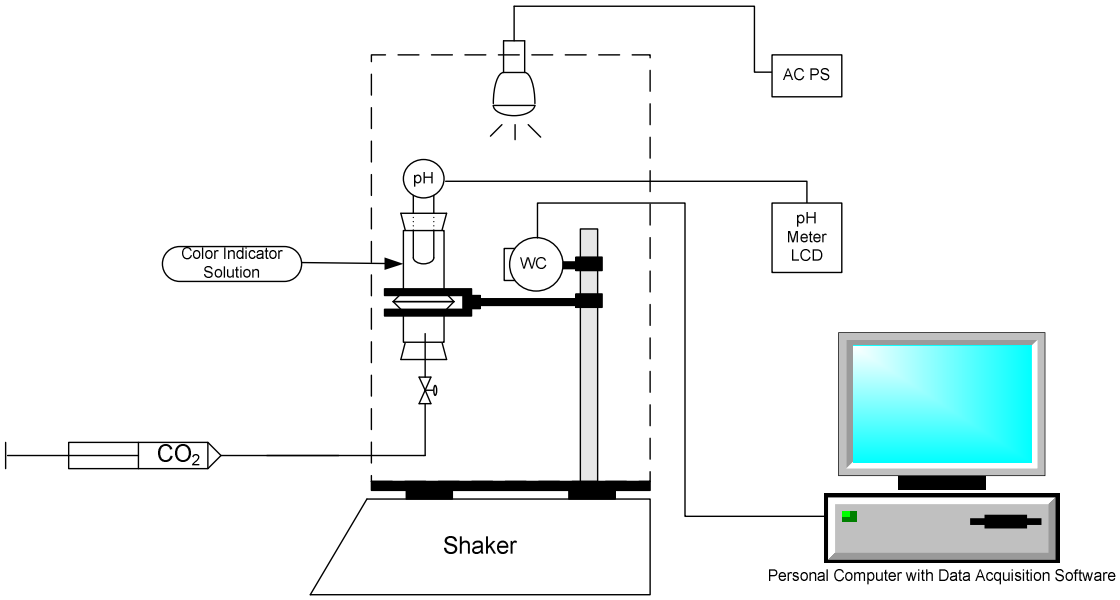

Figure 3.1: Testing apparatus for pH-color indicator solution

Figure 3.2: Photograph of testing apparatus for pH-color indicator solution

The same shaker table and foam poster board enclosure box was used as described in Chapter 2. However, a different light source was used. A General Electric fluorescent flood light bulb with a power of 11 watts and light output of 380 lumens was used to illuminate the inside of the box and provide a consistent light source.

A Harvard variable speed infusion/withdrawal pump (Model 600-900V) was used to propel the carbon-dioxide gas into the headspace below the indicator solution. TYGON R-3603 Laboratory tubing with an inside diameter of 3/8" was connected to a 10 ml syringe that was modified to fit in the carriage of the pump. A two-way valve was installed directly below the gaseous headspace of the membrane.

Indicator Solution

Triethanolamine (TEA) buffer solution was chosen for use in the indicator solution. The phenol red indicator was chosen because it changes from red to yellow between pH = 8.0

and pH =6.6. The indicator solution was prepared at room temperature (25^{o}C) and comprised of: 16.3 mM Triethanolamine Buffer Solution (Sigma-Aldrich, St. Louis, MO, U.S.), 30 µM phenol red, and de-ionized water.

Procedure

Dry ice was placed in a 250 ml beaker with approximately 10 ml of de-ionized water. Carbon dioxide (CO_2) gas was generated and the syringe was filled with CO_2 – rich gas. The syringe was connected to the tubing and CO_2 – rich gas was purged through the tubing to eliminate any ambient air. The end of the tubing was placed in the CO_2 – rich gas, the syringe was filled, and the valve was closed to prevent any gas leakage.

The tubing that was charged with CO_2 – rich gas was connected to the bottom of the chemical sensing apparatus in order to feed the gaseous headspace below the membrane. 18 ml of the pH-color indicator solution was placed onto the membrane. A stainless steel ball bearing with a diameter of 3/8” was placed in the solution on top of the membrane in order to break up surface tension at the membrane-liquid interface. The modified rubber stopper and pH meter were inserted into the pH-color indicator solution. The MATLAB software was used to select an area on the color indicator solution. A copy of the source code for the image acquisition software is attached in an appendix. For the sake of consistency, an area of 100 pixels x 100 pixels was selected each time. The recorded RGB value was the average value of all the pixels in the selected region. The value for red, green, and blue were recorded once every second. The enclosure box was placed on to the shaker and the shaker was turned on at a speed of 25 rpm. The system was allowed to equilibrate and the pH level was noted at the time that the MATLAB program began recording RGB values.

In order to add CO_2 gas to the solution, the shaker was stopped and the enclosure box was removed. The valve below the sensing apparatus was opened and 0.206 ml of CO_2 – rich gas was added to the gaseous headspace. The shaker was turned on while the CO_2 – rich gas was added in order to facilitate gas diffusion across the membrane. The valve was closed once CO_2 addition was complete and the enclosure box was replaced. The shaker was turned on and the pH was observed until it reached equilibrium. Once the pH reached equilibrium, the pH and time was noted and CO_2 – rich gas was added again. The color signal values for each data point were obtained by calculating the average of the data points taken for one minute (60 data points) when the pH measurement was taken. This procedure was repeated and replicated three times until ten data points (each with CO_2, pH, and RGB) were generated.

Results and discussion

Signal Processing and Sensor Calibration

The greatest change was seen in the green signal component of the RGB signal (Figure3.3).

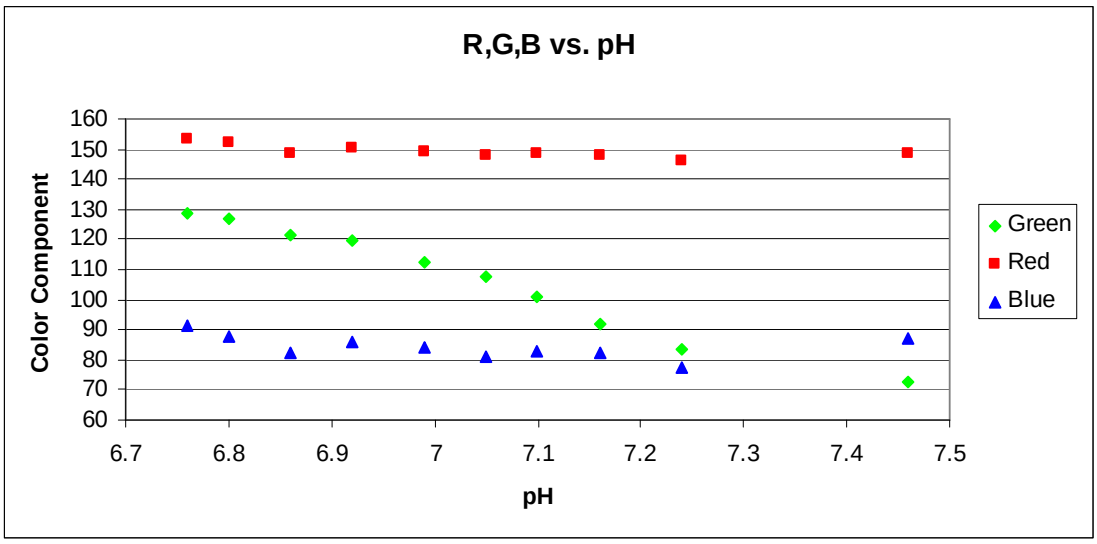

Figure 3.3: Individual color components recorded by CCD camera as a function of pH of indicator solution

The green signal was selected as the response signal to be used from the RGB values.

The change in pH of the indicator solution was highly correlated with the addition of CO_2 gas (R^2 = 0.9521, Figure 3.4).

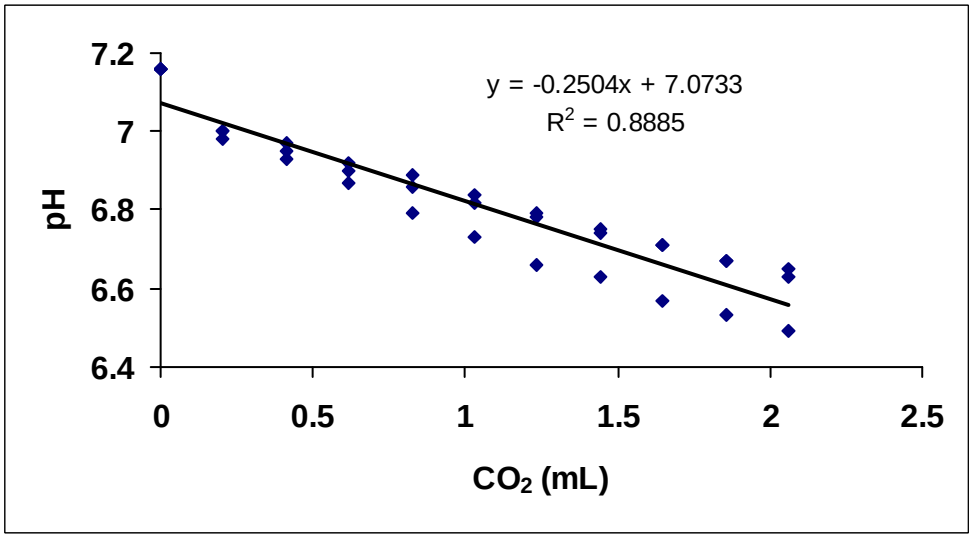

Figure 3.4: pH of indicator solution as a function of CO_2 added

The change in green signal detected by the CCD camera was highly correlated with pH change (R^2 = 0.968, Figure 3.5).

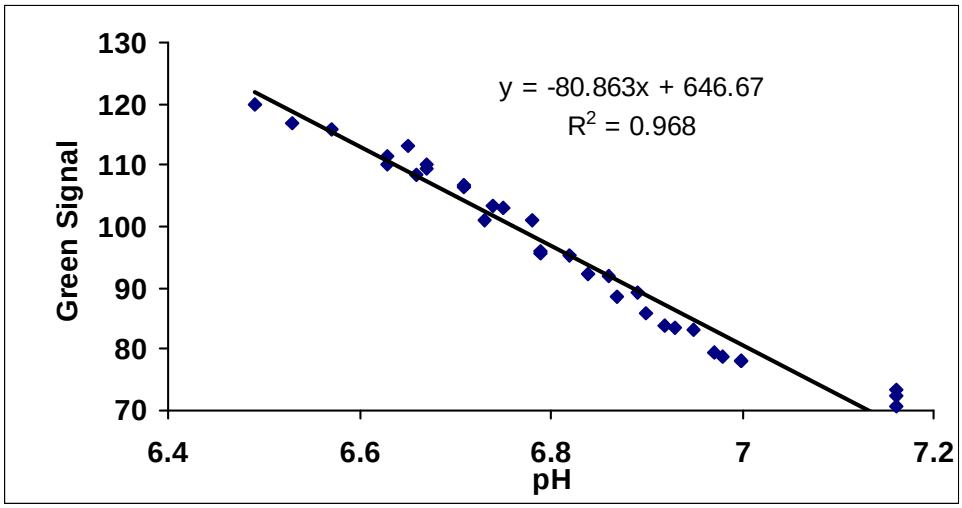

Figure 3.5: Green signal as a function of pH of indicator solution

A linear correlation was found between green signal change and CO_2 added (R^2 = 0.9418, Figure 3.6).

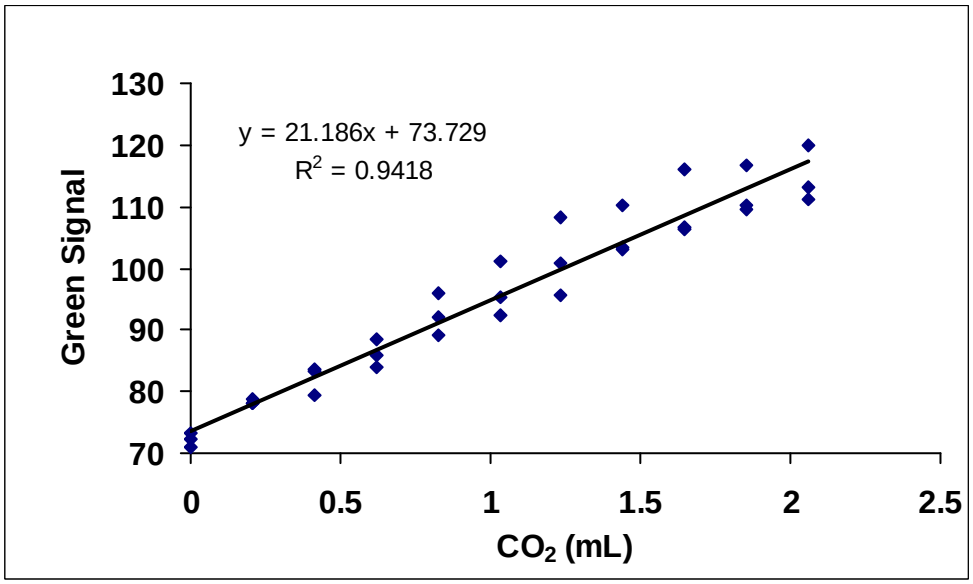

Figure 3.6: Green signal as a function of CO_2 added

The data was further processed to place the initial green value at zero. This is acceptable since the green signal change is relative to the initial detected value. The revised calibration is shown (Figure 3.7).

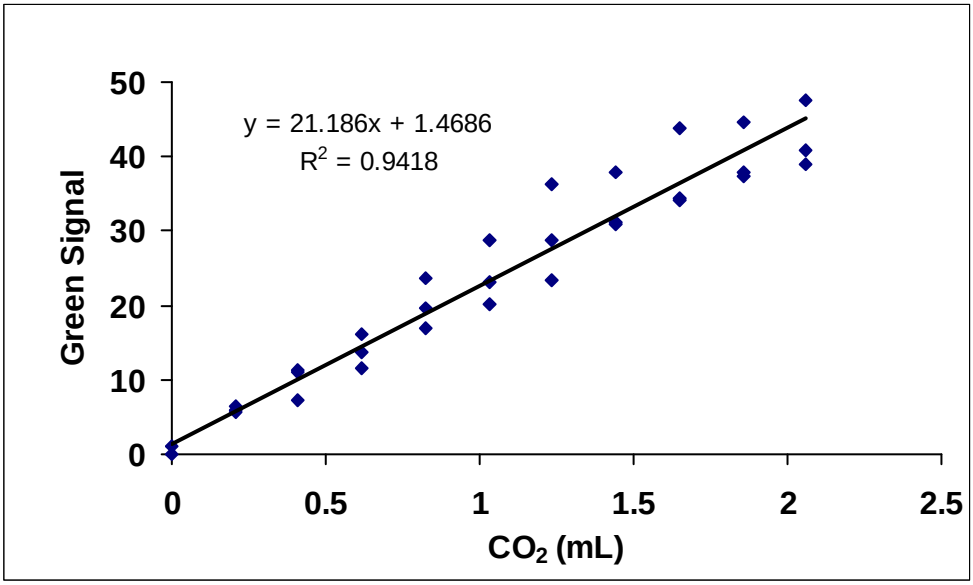

Figure 3.7: Green signal as a function of CO_2 added (Green signal values normalized to zero)

Conclusions

The addition of CO_2 into a buffered indicator was detected by change in color signal acquired by use of a CCD camera. The highest signal response was found to be in the green component of the RGB signal. The green signal should be used as the predictive indicator for color change in the indicator solution.

It also appears that the green signal is well correlated with CO_2 addition to the indicator solution. This is promising for developing the sensor for detecting CO_2 production from ethanol fermentations. It should be noted that the level of buffering capacity would likely need to be increased in order to be used on lab-scale fermentations since the level of

CO_2 production is much higher. These results indicate that the use of the described indicator solution, experimental apparatus, and CCD camera with data acquisition can be used to detect levels of CO_2 production as a function of color change.

CHAPTER 4.

Selection of Buffer Concentration for Glucose Fermentations

Introduction

The concept for the use of a chemi-visual sensor to detect CO_2 colorimetrically was described in Chapter 3. However, the CO_2 loadings used to develop and validate the concept were much lower than the expected CO_2 production from lab-scale fermentations. This chapter describes how the buffer concentration for glucose fermentations was developed.

Methods

A spreadsheet was designed to calculate the amount of expected ethanol and CO_2 production for given substrate loadings. The amount of CO_2 generated in the theory validation experiments was much lower than that for a typical glucose fermentation. A 125 mL Erlenmeyer flask was modified for use in fermentation monitoring experiments. A #15 glass o-ring joint was fused to the top of the flask and a sampling port with valve was fused near the base of the flask to enable sampling of fermentation broth while not allowing gas to escape. The valve was located below the level of the fermentation broth to ensure that no gas would escape due to sampling.

A series of experiments were conducted in order to find a suitable indicator solution. The goal was to find an indicator that would optimize the green signal change while for a given CO_2 loading. Based on the following calculations,

According to Varga, et al. (2004),

EtOH g = 1.045 CO_2 (g)

An optimistic estimate of conversion of glucose to ethanol was used:

0.50 g EtOH/g Glucose

Assume:

Ideal Gas Law: PV = nRT

Glucose = 1 g

Pressure = 1 atm

Molecular Weight CO_2 = 44.01 g/mol

Gas Constant (R) = 0.08206 (L - atm) / (^oK - mol)

Temperature = 310 ^oK

Then:

EtOH Produced (g) = (0.50 g EtOH/g Glucose) * (1.0 g Glucose)

EtOH Produced (g) = 0.50 g EtOH

CO_2 Produced (g) = 0.50 * 1.045

CO_2 Produced (g) = 0.52 g

Volume of CO_2 (mL) = ((0.52*0.08206*310)/(44.01*1)) * (1000 ml/L)

= 302.01 ml CO_2 produced

The phenol red buffer is designed to change from red at pH = 8.0 to yellow at pH = 6.6. With this in mind, a new indicator solution was prepared. The indicator solution was

prepared with 0.1 M TEA, 30 µM phenol red, and de-ionized water. The same experimental set-up was used as shown in Figure 3.1 as CO_2 generated by dry ice was added to the indicator solution.

The CO_2 was added 15 ml at a time and allowed to equilibrate for 5 minutes before recording the pH of the solution. RGB values were not recorded. The calibration curve for G = f(pH) (Figure 3.7) was used to estimate the amount of green signal change that could be expected.

Results and Discussion

The amount of green signal change achieved by the addition of 300 mL of CO_2-rich gas was near the lower detectable limits of the phenol red indicator range (Figure 4.1). A visual observation of the indicator solution confirmed that the solution appeared yellow at the end of the experiment and didn't appear to be changing color anymore.

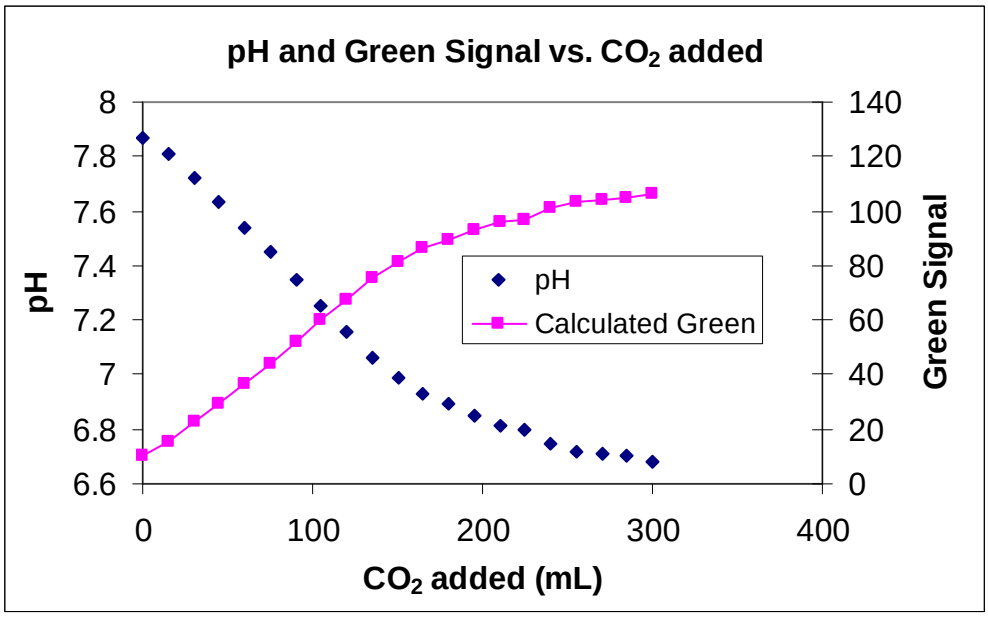

Figure 4.1: pH and green signal of indicator solution vs. CO_2 added to indicator solution

Green Signal Noise Due to Light Source

Introduction

Initial observations of the RGB data indicated a large amount of inherent variation in the RGB signal. A sinusoidal wave was detected in the RGB signal vs. time. It was hypothesized that the variation was due to the alternating current supply powering the light bulb. This section describes a series of experiments designed to ascertain and quantify the variation in the green signal.

Methods

An experiment was conducted to determine the effect of the light source on green signal variation. The green signal was monitored for the indicator solution with no fermentation being conducted. This was done in order to ascertain the inherent variation in the green signal due to the camera's detection and/or light source. The selected indicator solution (9 ml TEA, 7 ml D.I. H_2O, 2 mL phenol red solution) was used. The pH of the indicator solution was modified by addition of dilute sulfuric acid in order to read the green signal at low, middle, and high levels of the span of the green signal. An incandescent bulb with an AC light source (110 V) and a DC LED headlamp (3 V) were compared.

Results and Discussion

There was a large variation in the green signal that was illuminated by the AC light source (Figure 4.2). Much less inherent variation in the green signal was found with the DC LED light source.

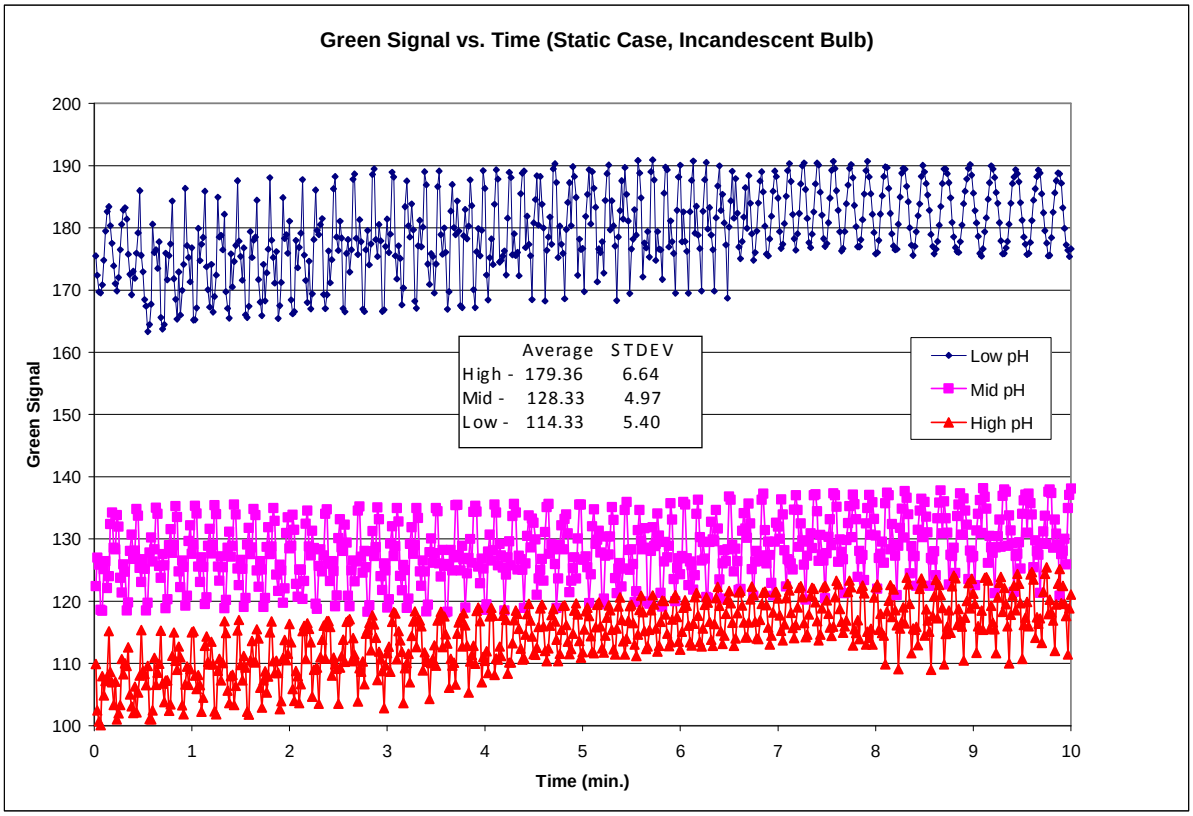

Figure 4.2: Green signal vs. time with a static indicator solution using the incandescent bulb as a light source

The variation seen in the green signal was significantly less for the case where the DC light source was used (Figure 4.3).

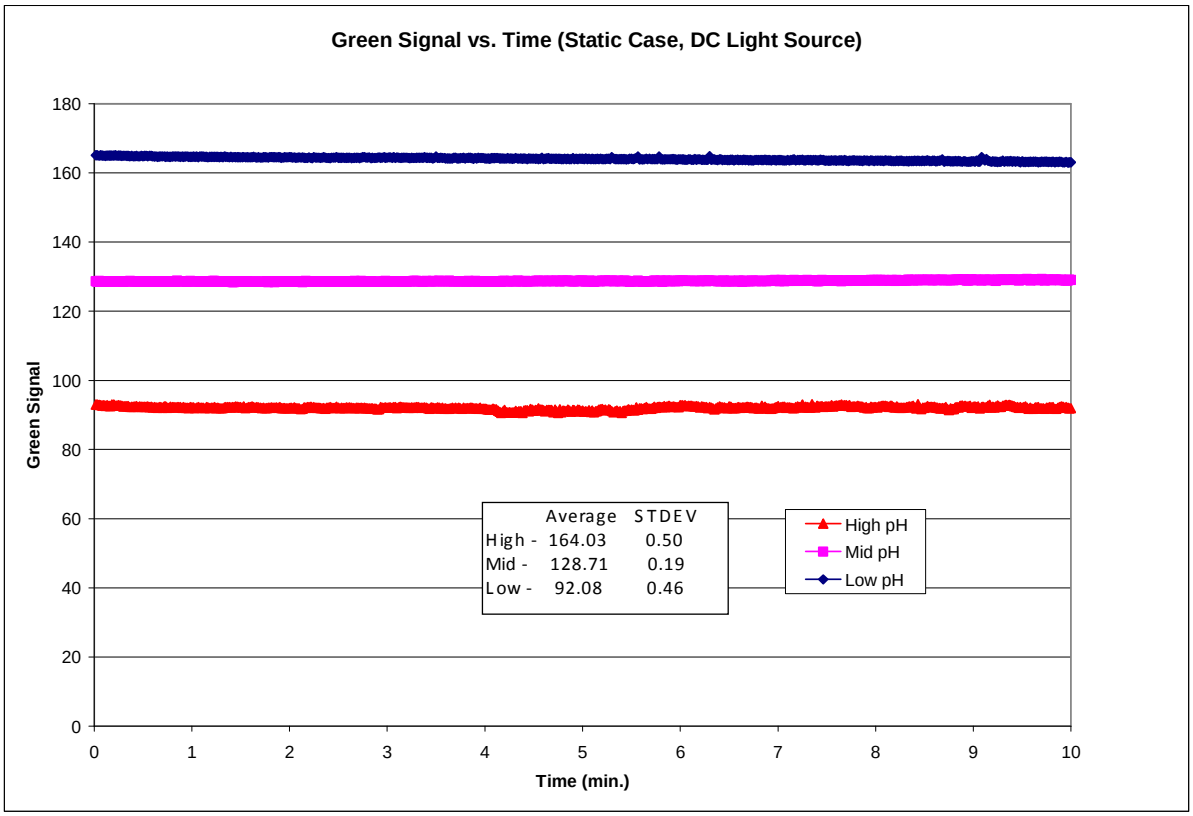

Figure 4.3: Green signal vs. time with a static indicator solution using the incandescent bulb as a light source

The observed disparity in variation of green signal due to light source is quite large. One possibility for the variation in green signal illuminated by the incandescent bulb is that the power supply is alternating current. The webcam is a very sensitive instrument and may be observing sinusoidal waves of the current source.

A 12 Volt /1.4 watt DC LED lamp (Sunlite Manufacturing, Brooklyn, NY) was chosen as the light source for the glucose fermentation experiments.

CHAPTER 5.

Fermentation Modeling

In an effort to determine the appropriate yeast loading for achieving a fermentation with a faster rate of ethanol production, a model of ethanol production was generated with an Excel spreadsheet. The model was based on previous work by Wang, et al. (2004) and used the following set of equations and parameters.

$$X = \frac{X_0 X_m e^{\mu_m t}}{X_m - X_0 + X_0 e^{\mu_m t}}$$

$$X_m = \left(Y_{x/s} S_0\right) + X_0$$

$$P = Y_{p/x}\left[\frac{X_0 X_m e^{\mu_m (t-\Delta t)}}{X_m - X_0 + X_0 e^{\mu_m (t-\Delta t)}} - \frac{X_0 X_m e^{-\mu_m \Delta t}}{X_m - X_0 + X_0 e^{-\mu_m \Delta t}}\right]$$

Where:

X = Biomass (yeast) concentration (g/L)

X_m = Maximum biomass (yeast) concentration (g/L)

X_0 = Initial biomass (yeast) concentration (g/L)

P = Ethanol production (g/L)

$Y_{p/x}$ = Yield coefficient of ethanol on biomass (g ethanol/g biomass)

$Y_{x/s}$ = Yield coefficient of biomass on sugar (g biomass/g sugar)

S_0 = Initial fermentable sugar concentration (g/L)

μ_m = maximum specific growth rate (h^{-1})

t = time (h)

Δt = lag time (h)

Ethanol fermentations were conducted at an initial yeast (X_0) loading of 1.5 g/L and S_0 of 15.3 g/L. The fermentation was sampled over a five hour period and ethanol concentration was determined using HPLC. Ethanol concentrations were determined as the average of three replicate samples. Three replicate experiments were performed and ethanol concentration data at each time point from the three experiments were averaged. Model parameters were estimated using the Excel Solver add-in to minimize the sum-square-error between the experimental data and the ethanol concentration predicted by the model.

Based on literature values, $Y_{x/s}$ for glucose was taken to be 0.22 (Wang, et al., 2004). Upper and lower limits for $Y_{p/x}$ (g/g) were taken to be 1.39 (Dantigny, 1995) and 5.57 (Wang, et al., 2004).

The values of μ_m, X_m, $Y_{p/x}$, and Δt were estimated by using an excel spreadsheet and using the solver add-in. to minimize the SSE. The upper and lower limits for $Y_{p/x}$ were used as a constraint as well. Figure 5.1 illustrates the output of the model using estimated parameter values.

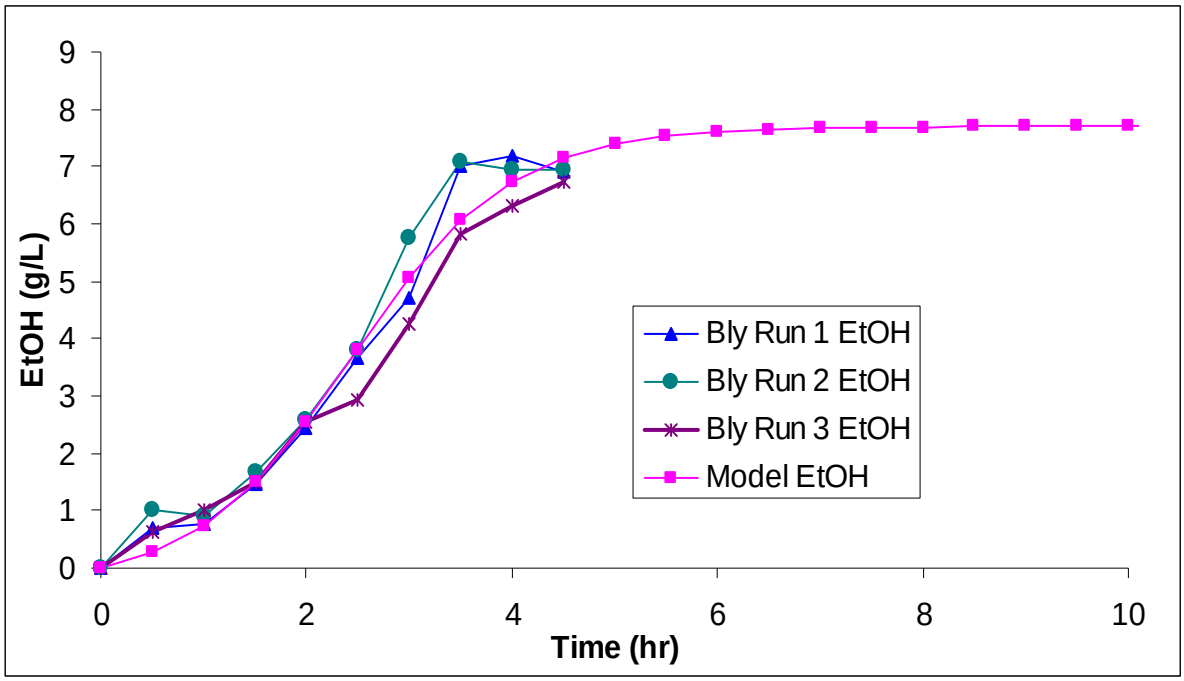

Figure 5.1: Response of ethanol production model

The estimated ethanol concentration predicted by the model matches the measured data well.

Table 5.2 outlines the estimated parameter values.

Table 5.2:Assumed and estimated values for ethanol production model

Model parameters	Value (units)	Source
$Y_{x/s}$	0.22 (g/g)	Wang et al. 2004
X_0	1.5 (g/L)	measured
$Y_{p/x}$	1.39 (g/g) - 5.57 (g/g)	Dantigny, 1995 & Wang et al. 2004
Estimated parameters		
X_m	7.388 (g/g)	estimated
$Y_{p/x}$	1.641 (g/g)	estimated
μ_m	1.293 (h^{-1})	estimated
Δt	1.82 (h)	estimated

The estimated values were used as fixed parameters in the same model while the yeast and glucose loading was varied in order to determine the proper yeast and glucose loading for a desired ethanol production rate.

Pressure Monitoring

System Set-up and Calibration

Pressure transducers from MSI Sensors (Part No. 1210A-100D-3L) were used to measure the pressure above the fermentation headspace and above the headspace of the indicator solution. A signal conditioning circuit with operational amplifiers was built in order to amplify the voltage measured by the pressure transducers. A detailed schematic is shown (Figure 5.2).

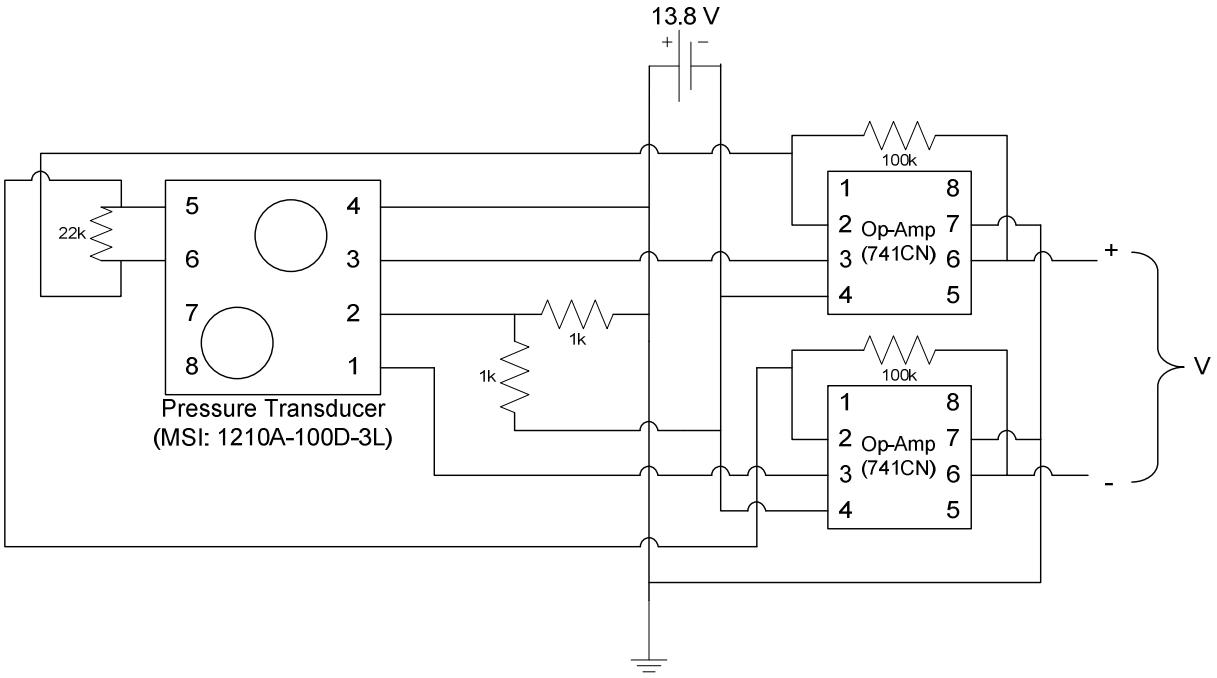

Figure 5.2: Schematic of signal conditioning circuit for pressure transducers used in pressure monitoring

The pressure transducers were calibrated using the setup shown in Figure 5.3.

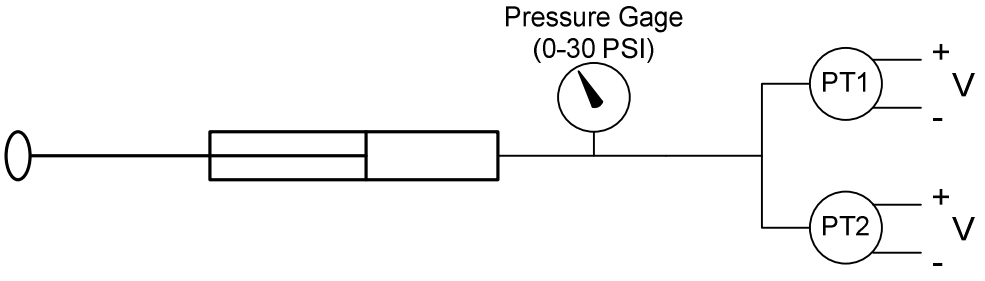

Figure 5.3: Set-up for calibration of pressure transducers

A bicycle hand pump was plumbed to the pressure transducers and used to alter the pressure to the pressure transducers. A dial pressure gauge (0-30 PSI) was used to observe the pressure applied to the pressure transducers. The amplified voltage signal was observed for each pressure transducer with a multi-meter for a range of pressures between 0 – 30 PSI. A calibration curve was developed by plotting pressure as a function of voltage (Figure 5.4).

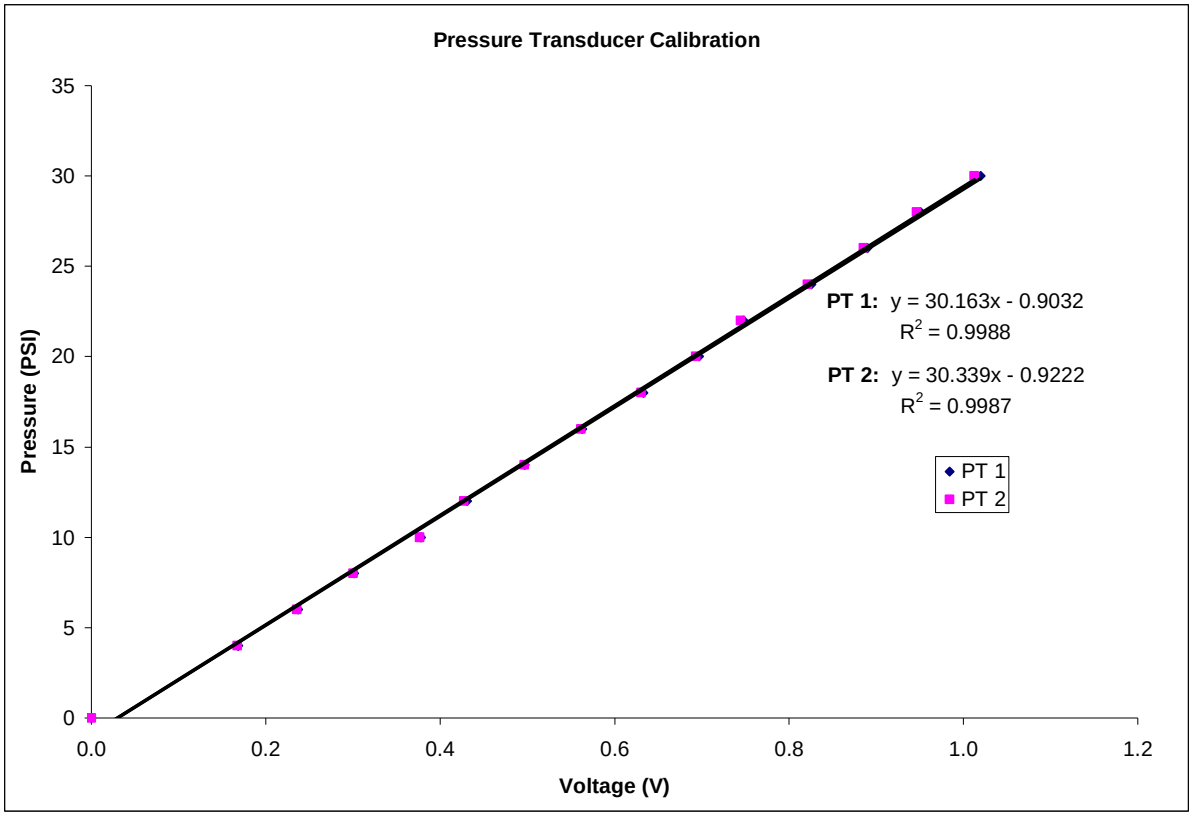

Figure 5.4: Calibration curve for MSI 1200D - 100L pressure transducers (PT1 = "Pressure Transducer 1" and PT2 = "Pressure Transducer 2")

Processing of Pressure Measurements

The pressure transducers were used to measure the pressure above the fermentation headspace and the headspace above the fermentation. A plot of pressure vs. time is shown (Figure 5.5).

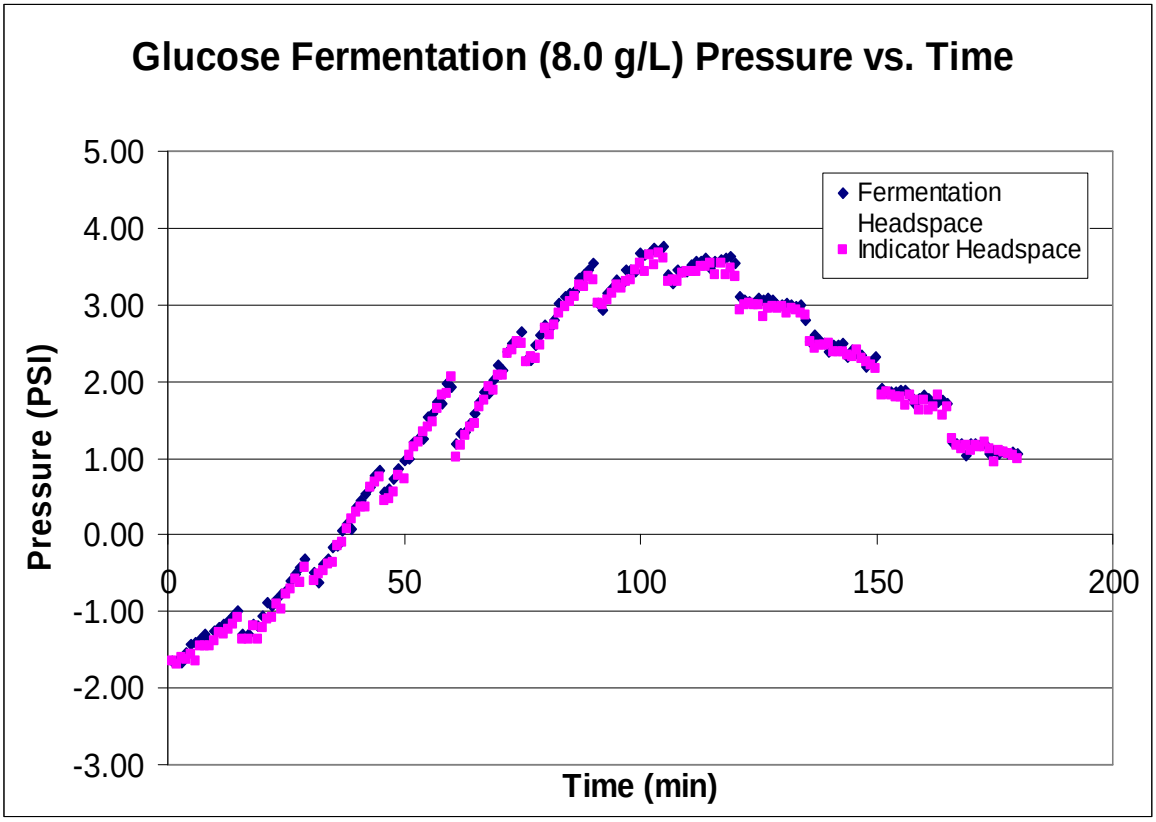

Figure 5.5: Pressure vs. time for fermentation with glucose loading of 8.0 g/L (Periodic drops reflect fermentation broth sampling)

The initial pressure shown for both the fermentation and indicator headspace locations are computed to be negative values based on the calibration equations. The initial pressure biases were eliminated and the subsequent pressure measurements adjusted by the same value in order to generate the following plot (Figure 5.6).

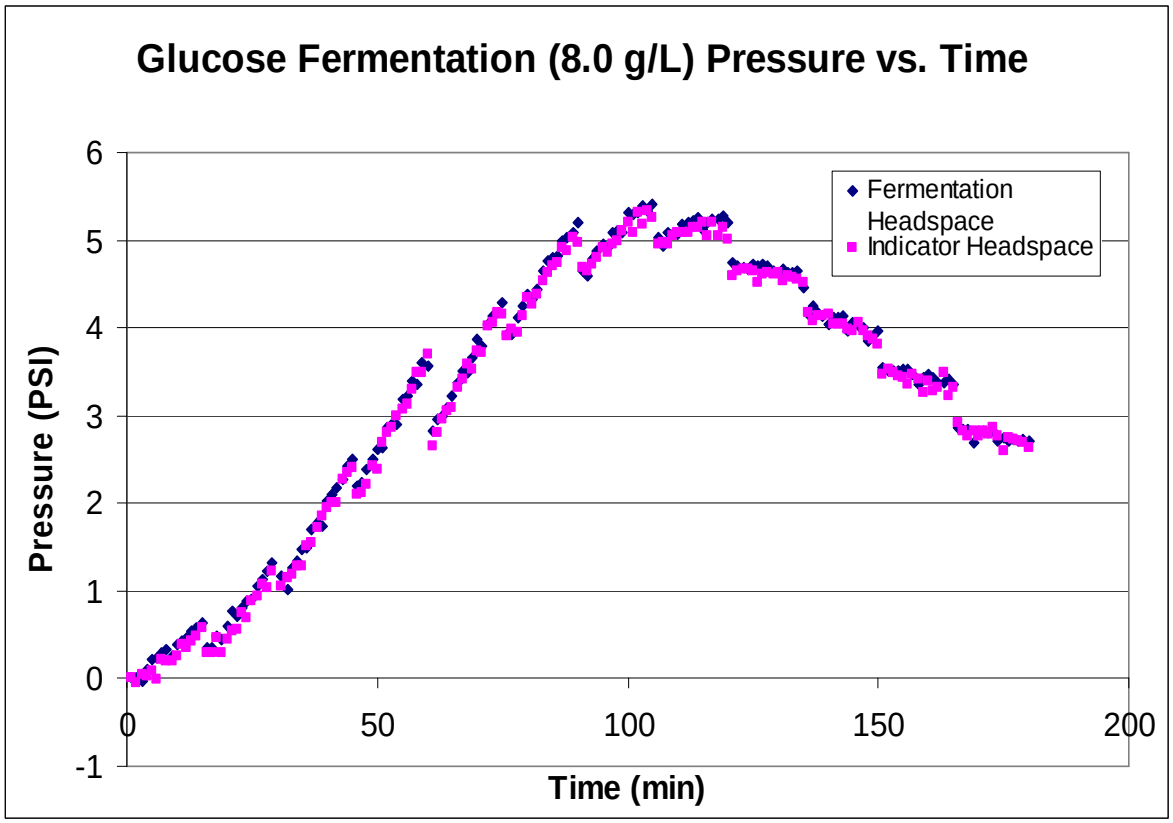

Figure 5.6: Pressure vs. time for fermentation with glucose loading of 8.0 g/L (Adjusted to make initial pressure measurement equal to zero)

There is an observed drop in pressure in the both pressure measurements at the time intervals when fermentation broth sampling occurs. For the fermentation shown, 2 mL of fermentation broth were removed every 15 minutes. Although the liberation of fermentation headspace gas was minimized by the location of the sample port, with each sample the broth volume was decreased increasing headspace volume and consequently a drop in observed headspace pressure. The pressure drop corresponding to the removed broth volume was computed and the data were corrected and the re-plotted in Figure 5.7.

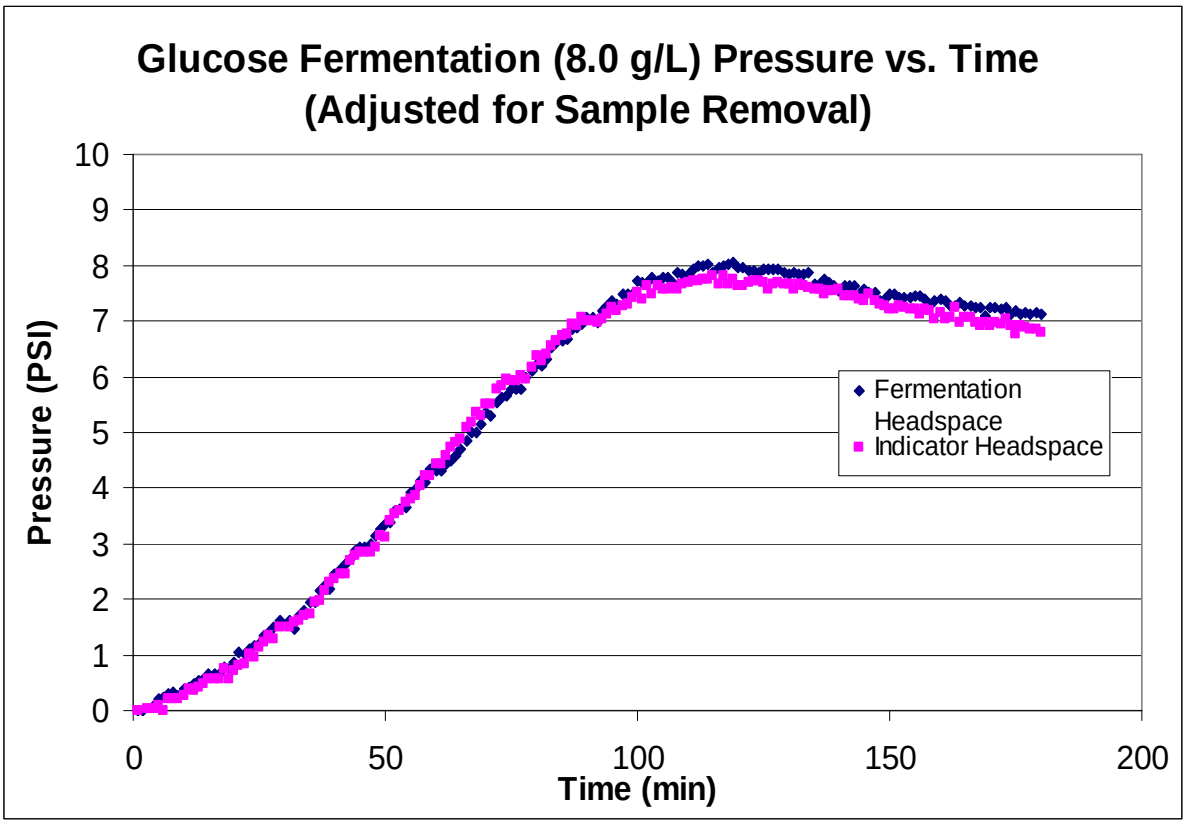

Figure 5.7: Pressure vs. time for fermentation with glucose loading of 8.0 g/L (Adjusted for volume increase due to sampling of fermentation broth)

The minimal difference in pressure between the fermentation headspace and indicator solution headspace can also be observed in Figure 5.8.

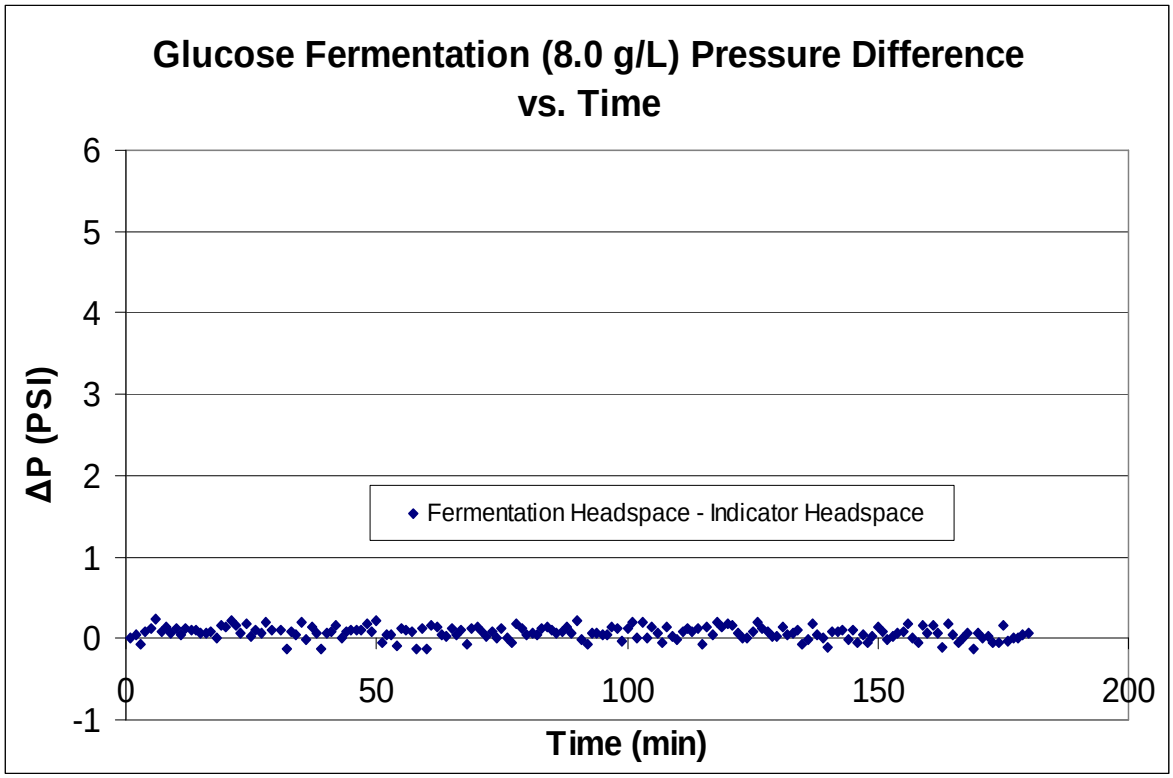

Figure 5.8: Pressure difference vs. time for glucose fermentation.

References

Dantigny, P. 1995. Modeling of the aerobic growth of *Saccharomyces cerevisiae* on mixtures of glucose and ethanol in continuous culture. Journal of biotechnology. 43: 213-220

Wang, D. Xu, Y., Hu, J., Zhao, G. 2004. Fermentation kinetics of different sugars by apple wine yeast *Saccharomyces cerevisiae*. Journal of the Institute of Brewing. 110: 340-346

CHAPTER 6.

GENERAL CONCLUSIONS

The purpose of this research was to develop and characterize a low-cost system to measure carbon dioxide gas produced during fermentation as a surrogate for ethanol production. A secondary objective was to evaluate the potential to miniaturize the sensing system to allow the monitoring of a large number of fermentations simultaneously.

The use of Triethanolamine (TEA) as a buffer to absorb CO_2 gas produced during fermentation was evaluated. Simple titrations with CO_2-rich gas indicate that a color change in the buffer should respond linearly to the addition of CO_2. The performance of the buffer at different fermentation kinetics was evaluated and non-linear responses in the green signal were observed for different ethanol production amounts. It was determined the TEA would not be an ideal choice for use as a buffer in sensing CO_2 gas production because of the un-wanted side reactions and non-linear responses for fermentations with different kinetics and substrate loadings.

The use of a phosphate buffer was further evaluated. A phosphate buffer was designed and the diffusivity of CO_2-rich gas into an open buffer system was found to be quite similar to the diffusivity of CO_2-rich gas into a buffer system with a membrane at the gas-liquid interface. It was calculated that the time required for the buffer to achieve 95% of full pH response for a given CO_2 addition is approximately 1 hour. The response of the sensor is greatly limited by the diffusion of CO_2 gas into the buffer.

The phosphate buffer system was evaluated for use in predicting ethanol production with observed green signal variations. It was found that the use of green signal change in the phosphate buffer solution as a predictor for ethanol production can account for approximately

92% of the change in actual ethanol content. The response of the green signal to ethanol production was slower for the fermentations with faster kinetics. The use of this sensor for estimating total ethanol production at the completion of fermentations would be more appropriate than using the sensor for predicting real-time ethanol concentrations.

The response of the sensor as it was tested is likely too slow to be accurate for monitoring fermentations that achieve full ethanol production at 2-4 hours like those evaluated in our experiments. However, if the kinetics of the fermentation were slower where full ethanol production was realized after 24-48 hours, the CO_2 evolution rate would be slower and the sensor would likely be more accurate in assessing real-time ethanol production.

Future work to develop this sensor should evaluate the potential increase in mass transfer by greater surface area of gas-liquid interface. A sensitivity analysis could be conducted to evaluate the interaction between buffer volume, fermentation headspace volume, and CO_2 production in order to optimize the system for potential miniaturization to enable screening of multiple samples simultaneously.